Shock wave profiles in the Burnett approximation

F. J. Uribe, R. M. Velasco, L. S. García-Colín, and E. Díaz-Herrera
Departamento de Física, Universidad Autónoma Metropolitana–Iztapalapa, 09340 México Distrito Federal, Mexico
(Received 26 May 2000)

This paper is devoted to a discussion of the profiles of shock waves using the full nonlinear Burnett equations of hydrodynamics as they appear from the Chapman-Enskog solution to the Boltzmann equation. The system considered is a dilute gas composed of rigid spheres. The numerical analysis is carried out by transforming the hydrodynamic equations into a set of four first-order equations in four dimensions. We compare the numerical solutions of the Burnett equations, obtained using Adam's method, with the well known direct simulation Monte Carlo method for different Mach numbers. An exhaustive mathematical analysis of the results offered here has been done mainly in connection with the existence of heteroclinic trajectories between the two stationary points located upflow and downflow. The main result of this study is that such a trajectory exists for the Burnett equations for Mach numbers greater than 1. Our numerical calculations suggest that heteroclinic trajectories exist up to a critical Mach number (≈ 2.69) where local mathematical analysis and numerical computations reveal a saddle-node–Hopf bifurcation. This upper limit for the existence of heteroclinic trajectories deserves further clarification.

PACS number(s): 47.40.Nm, 47.45.−n, 51.10.+y

I. INTRODUCTION

The problem of computing the structure of shock waves in fluids for a wide range of Mach numbers has been a perennial and debatable question in hydrodynamics. Until the late 1950s most of the work directed at elucidating the internal structure of a shock wave propagating in a fluid was based on the Navier-Stokes model of the continuum. As is well known, this model is based on the essential idea that the viscous tensor and the heat flux generated in the fluid due to a perturbation are expressed in terms of the deformation rate and the temperature gradient, respectively. The amount of work pursued along this line is enormous, too much to be mentioned in detail here. Excellent reviews and further references may be found in the literature [1–12]. The essence of the results obtained with the Navier-Stokes (NS) model as clearly summarized in Ref. [7] is that its validity is satisfactory for realistic fluids for Mach numbers (M) up to 1.8 but it definitely failed for $M>2$. If corrections of higher order in the gradients such as those provided by the Burnett equations were taken into account, it was more or less accepted that they would provide an improvement to the NS model for $M<1.8$ but they would worsen the results for $M\geqslant 2$.

On the other hand, the early 1950s also witnessed an entirely different approach to the study of shock wave profiles when, rather independently and using different ideas, Grad [13], Wang-Chang [14], and Mott-Smith [15] attempted to solve Boltzmann's equation describing the time evolution of a dilute monatomic gas. As is well known, the solution to this equation in the so-called hydrodynamic regime is equivalent to the NS model, except that the transport coefficients are obtained in terms of molecular parameters characteristic of each gas. After these works were published a host of papers appeared in the literature mostly devoted to assessment and clarification of the main ideas behind this kinetic theoretical way of viewing the problem. Nevertheless, and very likely as one should have expected, the general trend of the results obtained with the NS continuum model remained unchanged. The Mott-Smith results rated a little better than those obtained with Grad's 13-moment method or with the Chapman-Enskog method for solving the Boltzmann equation, but the assumptions made are physically not very convincing. Once more, for further details we refer the reader to the vast literature available [15–24]. Three main lines of thought that played an important role in the development of the subject arose from this effort. The first one is related to the existence of kinetic theory solutions to the shock wave problem. In his 1952 paper, Grad [13] already asserted that it was unlikely that the 13-moment solution to the Boltzmann equation correctly determined the thickness of a shock wave for $M\approx 1.61$. A few years later, Holway presented a proof claiming that for Grad's moment method of solving Boltzmann's equation there exists a critical value of M (≈ 1.851) for which no continuous shock solution is possible [25]. This statement was emphasized by Ruggeri only a few years ago [26] and claimed by Weiss to be incorrect [27]; there is no such upper bound of M for which a solution exists. This result is closely connected with the second line of thought as we shall argue below.

The standard method of solving the Boltzmann equation is based on a perturbation scheme known as the Chapman-Enskog method [28]. The essential idea consists of expanding the single particle distribution function around the local equilibrium state in powers of Knudsen's parameter (K), which in the case of shock waves is defined as the ratio between the mean free path and the thickness of the shock. For weak shocks this number is smaller than 1, so that it is logical to expect that the first correction to the local equilibrium state that leads to the NS equations is good enough to correctly describe shock wave profiles. In spite of the results already mentioned above, namely, that the NS regime is satisfactory only for weak shocks, many authors in the field set out to explore how the next order corrections to such a parameter would modify the existing results. This has led to a long standing and controversial question concerning the validity and usefulness of the Burnett and super-Burnett equa-

tions in the description of shock wave profiles. Although first sketched by Wang-Chang in his paper on the subject [14] it was throughly examined by Foch [29] and later by many other workers in the field [30–34]. The conclusions of these reports are not altogether consistent with each other. For some authors the Burnett corrections to the NS regime are important, for example Chapman *et al.* [32–34] reported agreement with Monte Carlo results up to $M \approx 50$. We shall come back to this question later.

Finally the third line of thought has been to use Enskog's kinetic equation, valid for a dense fluid of rigid spheres, to examine shock wave structures in both the NS and the Burnett regimes [35,36]. Although this work is somewhat foreign to the subject of this paper the results that have been obtained merit a closer examination especially because one should expect compatibility with those obtained for the dilute gas.

Calculation of shock wave profiles in dilute gases as well as in dense fluids has also been greatly benefited by the advent of modern computational techniques such as the direct simulation Monte Carlo (DSMC) method [37], nonequilibrium molecular dynamics (NEMD) [38], powerful numerical methods for integrating linear and nonlinear differential equations [39–42], and computer algebra [43]. NEMD calculations for shock waves were published in 1980 by Holian *et al.* [44]. There, a steady strong shock wave propagating in a dense fluid was simulated and the relevant profiles compared with those obtained from the NS continuum model. The main results that emerged from that work were later brought into a more refined theory by Holian himself. This theory is based on the idea that along the direction of propagation of the shock wave there are two different temperatures, one along this direction and a second one in the plane perpendicular to it. Since the viscosity and thermal conductivity depend on the temperature, it is conjectured that they should depend only on the parallel temperature. This conjecture [45,46], now referred to as Holian's conjecture, has defied any microscopic interpretation [47] but has provided an improvement in the agreement between continuum models and numerical simulations [46]. A breakthrough in this approach to the problem occurred in 1992 when Salomons and Mareschal [48] used both NEMD and the DSMC method to compute shock wave profiles in a dilute hard sphere gas in the range $4 \leqslant M \leqslant 134$. The main objective of the work was to investigate the accuracy of the Burnett equations for $M > 2$ in a dilute gas by computing the fluxes present in the gas, not the profiles obtained by a full hydrodynamic calculation. Their main result was that in such a regime and even at such large M's the improvement on Fourier's law is substantial. Curiously enough, a few months later a communication by these authors and Holian's group was published [49] modeling shock waves in ideal fluids using Holian's theory and exhibiting the improvement of this theory as compared with the NS model, leaving aside completely the previous claim about Burnett's approximation. This completes the description of the general background that inspired our work and which we now report in some detail in this paper. A previous short Letter is already available in the literature [50].

We shall here restrict ourselves to the discussion of what is really the importance of the Burnett constitutive equations in the calculation of shock wave profiles in dilute gases for Mach numbers greater than or equal to 2. Two questions, at least, jump to the fore. The first one is concerned with the improvement in the structure of shock waves. The second one is related to the justification of such an improvement, if it truly exists, based on more basic principles. Indeed, it would be hard to accept that the Chapman-Enskog method, which provides a power series for the distribution function in terms of the magnitude of the gradients in the system, provides reliable results for strong shock waves. In this paper we shall be solely concerned with the first question. For that purpose we shall integrate the full hydrodynamic equations in the nonlinear Burnett approximation for a simple dilute gas and show that the shock wave profiles in the range covered in Ref. [47] are substantially improved, with respect to both the NS model and Holian's theory. The second question, which became quite relevant in the light of the results obtained here, will be dealt with elsewhere.

To present the results we have structured our paper as follows. In Sec. II a statement of the problem will be given. Section III is devoted to a discussion of the methods used in solving the nonlinear set of differential equations as well as the results obtained with the DSMC method. Section IV is concerned with a discussion of the relevant mathematical aspects of the problem. Finally, in Sec. V we will give some concluding remarks.

II. THE PROBLEM

Our interest lies in the study of a traveling wave that propagates with constant velocity c, assuming that two equilibrium states are possible. For simplicity we will assume that we are dealing with a plane wave so that the velocity of the perturbation, which we denote by $\mathbf{u} = u(x,t)\mathbf{i}$, has a component along the x direction, and that furthermore the velocity of the perturbation can depend only on x and t. The equations that describe the evolution of the hydrodynamic variables are given by the conservation equations, which read

$$\frac{\partial}{\partial t}\rho(x,t) + \frac{\partial}{\partial x}[u(x,t)\rho(x,t)] = 0, \tag{1}$$

$$\frac{\partial}{\partial t}u(x,t) + u(x,t)\frac{\partial u(x,t)}{\partial x} = -\frac{1}{\rho(x,t)}\frac{\partial}{\partial x}(\mathbf{P}_{xx}), \tag{2}$$

$$\frac{\partial}{\partial t}e(x,t) + u(x,t)\frac{\partial}{\partial x}[\rho(x,t)e(x,t)] = -\mathbf{P}_{xx}\frac{\partial u(x,t)}{\partial x} - \frac{\partial}{\partial x}(\mathbf{q}_x), \tag{3}$$

where ρ is the mass density, $\mathbf{P}_{xx}$ the xx component of the pressure tensor, e the specific internal energy, and $\mathbf{q}_x$ the x component of the heat flux. The explicit equations that describe the behavior of the hydrodynamic variables are obtained when the constitutive relations are given. They can be the Euler equations, the Navier-Stokes-Fourier equations, or the Burnett equations among many others. Let $\Psi(x,t) = (u(x,t), \rho(x,t), T(x,t), e(x,t), \mathbf{P}_{xx}(x,t), \mathbf{q}_x(x,t))$; then the interest is in finding traveling wave solutions of the form

$\Psi(x,t)=\phi(x-ct)$. Since the velocity c is assumed to be constant then, provided that such a solution exists, it is possible to choose a coordinate system moving with velocity c so that the shock wave is stationary and Ψ does not depend on time. In the case of the Euler equations it is known that a continuous curve joining the two equilibrium points does not exist and it is necessary to consider weak solutions to the equations. We again refer the reader to the mathematical literature that deals with such solutions [51–53]. Rayleigh [54] and Taylor [55] showed that in order to have a smooth curve joining the two equilibrium points it is necessary to introduce the transport coefficients into the description of the shock wave. For example, if we use the Navier-Stokes-Fourier (NSF) linear constitutive equations the viscosity and thermal conductivity play a role and it is here that the information about the intermolecular potential comes in. According to Liu [56], it was Stokes in 1848 who first pointed out the need to introduce the transport coefficients in order to have a continuous curve joining the two equilibrium points. The Navier-Stokes-Fourier linear constitutive equations give expressions for $\mathbf{P}_{xx}$ and $\mathbf{q}_x$ in terms of p, T, u, and some of their first-order derivatives so that the integrated form of the conservation equations gives rise to two ordinary differential equations with boundary conditions, which have been studied extensively [3]. But other relations such as the Burnett constitutive equations may be considered, and as we will show here they turn out to be more adequate when large gradients are present such as happens in shock waves.

The problem can also be considered from the point of view of the Boltzmann equation [22,57–59], which is more fundamental than studying approximate solutions to the Boltzmann equations such as those provided by the Chapman-Enskog method. In this case the single particle distribution function is assumed to be of the form $f(x,\mathbf{v},t)=f(x-ct,\mathbf{v})$, where $\mathbf{v}$ is the atomic velocity, so it follows that $\Psi(x,t)=\phi(x-ct)$ and in particular the relevant moments correspond to a traveling wave. In the final section we will provide a discussion of the results of such an approach.

A. The conservation equations

We are interested in describing a one dimensional stationary shock wave according to a continuum approach. The conservation equations of mass, momentum, and energy for a one dimensional stationary system can be readily obtained from Eqs. (1)–(3), namely,

$$\frac{\partial}{\partial x}[u(x)\rho(x)]=0, \tag{4}$$

$$u(x)\frac{\partial u(x)}{\partial x}=-\frac{1}{\rho(x)}\frac{\partial}{\partial x}(\mathbf{P}_{xx}), \tag{5}$$

$$u(x)\frac{\partial}{\partial x}[\rho(x)e(x)]=-\mathbf{P}_{xx}\frac{\partial u(x)}{\partial x}-\frac{\partial}{\partial x}(\mathbf{q}_x). \tag{6}$$

Equations (4)–(6) can be integrated to give

$$\rho(x)u(x)=C_1, \tag{7}$$

$$\rho(x)u^2(x)+\mathbf{P}_{xx}=C_2, \tag{8}$$

$$\left(e(x)+\frac{1}{2}u^2(x)\right)\rho(x)u(x)+\mathbf{P}_{xx}u(x)+\mathbf{q}_x=C_3, \tag{9}$$

where C_1, C_2, and C_3 are constants. In the shock wave problem it is assumed that there exist two equilibrium states, characterized by the fact that there are no gradients, so that $\mathbf{P}_{xx}=p$, where p is the pressure and $\mathbf{q}_x=0$. Such equilibrium states are denoted as upflow and downflow states, corresponding to the higher and lower values of u, respectively. The constants can be determined in terms of any set of equilibrium values, and the result can be written in the form

$$\rho_U u_U=\rho_D u_D=C_1,$$

$$\frac{\rho_U}{2}u_U^2+p_U=\frac{\rho_D}{2}u_D^2+p_D=C_2,$$

$$\left(e_U+\frac{1}{2}u_U^2\right)+p_U u_U=\left(e_D+\frac{1}{2}u_D^2\right)+p_D u_D=C_3. \tag{10}$$

This set of equations constitute the well known Rankine-Hugoniot jump conditions. When the values of the mass density, pressure, and velocity at either the upflow or downflow state are given then the values at the other equilibrium point can be determined. Up to now Eqs. (4)–(10) are not restricted to the dilute case and they are valid for any intermolecular potential. For a dilute gas we have that $p=nkT$, where n is the number density, k Boltzmann's constant, and T the temperature. Also, we have that $e=3/2kT$ for a gas without internal degrees of freedom.

B. The Navier-Stokes dynamical system

We begin by considering the Navier-Stokes-Fourier linear constitutive equations that are obtained as the first-order term in the Knudsen expansion of the Chapman-Enskog method [28]. In order to calculate the viscosity and thermal conductivity we will consider the rigid sphere model. The main reason to consider this model is that the interaction is known and we do not have to determine the true interaction potential (in case we were interested in experimental data); in addition, the mean free path is well defined and the model is more akin to the ideas used by Boltzmann to deduce his equation [28,60]. For the case of a shock wave, the general results [28] for the constitutive equations reduce to

$$\mathbf{P}_{xx}=p(x)-\frac{4}{3}\mu\frac{du}{dx}, \tag{11}$$

$$\mathbf{q}_x=-\lambda\frac{dT}{dx}. \tag{12}$$

μ is the viscosity and λ the thermal conductivity, which for the rigid sphere model are given by [28]

$$\mu=\frac{5c_\mu}{16\sigma^2}\left(\frac{mkT(x)}{\pi}\right)^{1/2},\quad \lambda=\frac{75c_\lambda}{64\sigma^2}\left(\frac{k^2T(x)}{\pi m}\right)^{1/2}, \tag{13}$$

where σ is the rigid sphere diameter and to first order in the Sonine expansion the coefficients c_μ and c_λ are equal to 1. Exact values for them can be found in the book by Chapman

and Cowling [28]. In this work we take $c_\mu = c_\lambda = 1$; the results for the different profiles considered are not affected in a measurable way if their exact values are used.

It is convenient to express the differential equations in the Navier-Stokes regime in reduced form and we will follow the definition given by Holian *at al.* [49]. Moreover, we will also use their notation, which consists in denoting the quantities at upflow by the subindex zero and the quantities at downflow by a subindex 1. Accordingly, the reduced speed $u^\star(s)$ and temperature $\tau(s)$ are defined by

$$s \equiv x/l, \quad l = \frac{5m}{12\rho_0\sigma^2\sqrt{\pi}}, \quad \tau(s) \equiv \frac{kT(x)}{mu_0^2}, \tag{14}$$

$$u^\star(s) \equiv u(x)/u_0, \quad \tau_0 \equiv \frac{p_0}{\rho_0 u_0^2}.$$

The integrated form of the conservation equations given by Eqs. (8) and (9) can be rewritten as

$$\mathbf{P}_{xx}^\star = \tau_0 + 1 - u^\star(s), \tag{15}$$

$$\frac{3}{2}\tau(s) + \mathbf{q}_x^\star = \frac{3}{2}\tau_0 + \frac{1}{2}[1-u^\star(s)]^2 + \tau_0[1-u^\star(s)], \tag{16}$$

where $\mathbf{P}_{xx}^\star \equiv \mathbf{P}_{xx}/\rho_0 u_0^2$ is the reduced xx component of the pressure tensor and $\mathbf{q}_x^\star \equiv \mathbf{q}_x/\rho_0 u_0^3$ the reduced x component of the heat flux. To obtain Eqs. (15) and (16) the integrated form of the mass conservation equation, given by Eq. (7), was used. Holian *et al.* [49] chose the origin of s in such a way that the reduced velocity at $s=0$ gives the average of the upstream and downstream values for $u^\star$ and the solution of the equations that we will consider (NS, Holian and Burnett) depends on this choice. However, the profiles obtained for different choices of the origin come together when they are translated along s, reflecting the fact that the equations are invariant under the choice of the origin for s. Thus, they exhibit translational symmetry. A similar behavior has been noted in the shock profiles obtained by the DSMC method [37].

The governing equations for the Navier-Stokes regime are obtained by calculating $\mathbf{P}_{xx}^\star$ and $\mathbf{q}_x^\star$ from Eqs. (11) and (12) and by direct substitution of these expressions in Eqs. (15) and (16) we arrive at

$$\frac{\tau(s)}{u^\star(s)} - \tau^{1/2}(s)u^{\star\prime}(s) = \tau_0 + 1 - u^\star(s),$$

$$\frac{3}{2}\tau(s) - \frac{45}{16}\tau^{1/2}(s)\tau'(s) = \frac{3}{2}\tau_0 + \frac{1}{2}[1-u^\star(s)]^2 + \tau_0[1-u^\star(s)]. \tag{17}$$

Here the prime denotes the derivative with respect to s. Equations (17) can be solved for the derivatives of $u^\star$ and τ to give

$$u^{\star\prime}(s) = \frac{1}{\tau^{1/2}(s)}\left(\frac{\tau(s)}{u^\star(s)} - \tau_0 - 1 + u^\star(s)\right),$$

$$\tau'(s) = \frac{16}{45\tau^{1/2}(s)}\left(\frac{3}{2}\tau(s) - \frac{3}{2}\tau_0 - \frac{1}{2}[1-u^\star(s)]^2 - \tau_0[1-u^\star(s)]\right). \tag{18}$$

The system of two equations with two unknowns given by Eqs. (18) has to be solved for certain boundary conditions which can be obtained from the Rankine-Hugoniot jump conditions given by Eqs. (10). The result is given by

$$u_1^\star = \frac{5}{4}\tau_0 + \frac{1}{4}, \quad \tau_1 = \frac{7}{8}\tau_0 + \frac{3}{16} - \frac{5}{16}\tau_0^2, \quad u_0^\star = 1. \tag{19}$$

Notice that these boundary conditions are written in terms of τ_0, the reduced temperature in the upflow state. This quantity is related to the Mach number (M), which is defined as the ratio of the velocity of the shock at upflow and the adiabatic sound velocity at upflow, by the relation

$$M = \sqrt{\frac{3}{5\tau_0}}, \tag{20}$$

where the ratio of the specific heat at constant pressure divided by that at constant volume is taken to be 5/3, as it should be for a classical gas without internal degrees of freedom.

It is a common practice in the literature to divide the first equation of Eqs. (18) by the second one and obtain only one first-order differential equation, but it is also possible to treat the whole dynamical system given by Eqs. (18) as is done here. Since the calculations for such two dimensional dynamical systems are simple and the results are well known [3,13], we will mention only what we found. The upstream critical or stationary point $(1,\tau_0)$ is an unstable node and the downstream critical point (u_1,τ_1) is a saddle. This is, of course, in agreement with known results and in fact it has been known for a long time that there exists a unique differential curve joining the critical points $(1,\tau_0)$ and (u_1,τ_1) [3]. In the mathematical literature a curve connecting two critical points is referred to as a heteroclinic trajectory so we will adopt this terminology. Following Holian *et al.* [49], we assume that the upstream critical point is obtained when $s \to -\infty$ and the downstream one when $s \to \infty$. In this case and due to the topological nature of the stationary points the solution curve must go from the saddle to the unstable node, which becomes a stable node since the integration with respect to s goes in the negative direction, that is, s varies from positive to negative values. The topological nature of the stationary points also provides us with a practical way to obtain the solution numerically, a method used long ago by Gilbarg and Paolucci [3]. In modern terminology it can be expressed as follows. One perturbs the downstream stationary point and integrates numerically toward $s \to -\infty$; then, when the perturbed point is in the basin of attraction of an invariant set, the numerical solution will be attracted to it and it will give an approximate solution to the problem, that is,

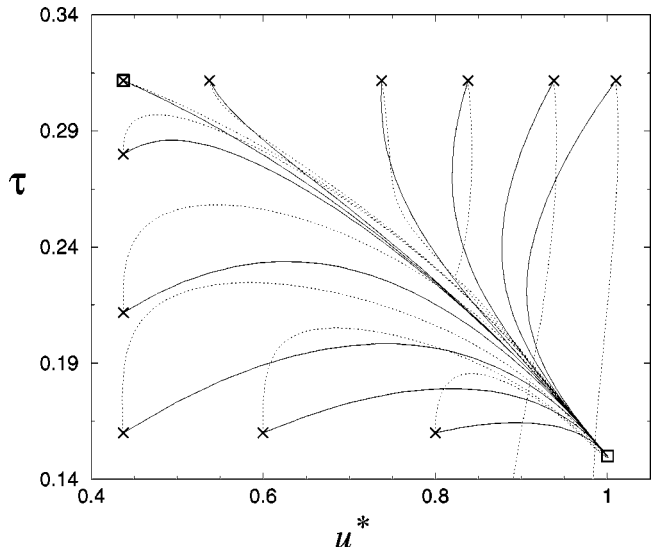

FIG. 1. Orbits in the $u^\star$-τ plane for $M=2$ and different initial values. Squares, critical points; solid line, Navier-Stokes; dotted line, Burnett; crosses, initial points.

the heteroclinic trajectory will emerge. Holian *et al.* [49] noted that it was sufficient to perturb the downstream velocity by making it a little higher than its asymptotic value in order that the perturbed point be in the basin of attraction of an invariant set, although they reported the calculations only for $\tau_0=0$ $(M=\infty)$. On the other hand, other authors [35] and we ourselves [47] have used the procedure by Holian *et al.* to numerically generate the profiles for finite Mach numbers and in fact the same procedure worked out for the Burnett equations [50]. Figure 1 shows the integral curves of the dynamical system given by Eq. (18) for different initial values and $M=2.0$. In this case we have also considered initial conditions far from downstream to show that the solutions generated numerically are attracted to the heteroclinic trajectory whose numerical approximation corresponds to the orbit generated by the initial condition that is very near the upstream critical point.

C. The Burnett dynamical system

The Chapman-Enskog [28] expansion generates the contributions to the fluxes at different orders in the Knudsen number. The zero-order term in the Knudsen number, which corresponds to a nonviscous fluid, gives the following values for the pressure tensor and heat flux:

$$\mathbf{P}^{(0)}=p\mathbf{I}, \quad \mathbf{q}^{(0)}=\mathbf{0}, \tag{21}$$

where $\mathbf{I}$ is the unit tensor. Substitution of the previous constitutive relations in the conservation equations (4)–(6) gives the Euler equations. To first order in the Knudsen number, which corresponds to the second-order term in the Chapman-Enskog expansion, the corresponding expressions are

$$\mathbf{P}^{(1)}=-2\mu\overset{\circ}{\overline{\overline{\nabla\mathbf{c}_0}}}, \quad \mathbf{q}^{(1)}=-\lambda\nabla T, \tag{22}$$

where the double overbar denotes the symmetric tensor, the overcircle denotes the corresponding traceless tensor [28], and $\mathbf{c}_0$ is the hydrodynamic velocity. In the Navier-Stokes regime the total pressure tensor, meaning the contributions up to first order in the Knudsen number, is the sum of $\mathbf{P}^{(0)}$ and $\mathbf{P}^{(1)}$ with an analogous result for the heat flux. When $\mathbf{c}_0=u(x)\mathbf{i}$ the result for $\mathbf{P}^{NS}\equiv\mathbf{P}^{(0)}+\mathbf{P}^{(1)}$ reduces to the expression given in Eqs. (11), and similarly for the heat flux.

The contribution to second order in the Knudsen number or the third-order term in the Chapman-Enskog expansion has been calculated by Burnett [61] (see also Chap. 15 in Ref. [28]) and the results can be expressed in the form

$$\begin{aligned}\mathbf{P}^{(2)}=&\omega_1\frac{\mu^2}{p}\Delta\mathring{\mathbf{e}}+\omega_2\frac{\mu^2}{p}\left\{\frac{D_0}{Dt}\mathring{\mathbf{e}}-2\overset{\circ}{\overline{\overline{\nabla\mathbf{c}_0\cdot\mathring{\mathbf{e}}}}}\right\}+\omega_3\frac{\mu^2}{\rho T}\overset{\circ}{\overline{\overline{\nabla\nabla T}}}\\&+\omega_4\frac{\mu^2}{\rho pT}\overset{\circ}{\overline{\overline{\nabla p\nabla T}}}+\omega_5\frac{\mu^2}{\rho T^2}\overset{\circ}{\overline{\overline{\nabla T\nabla T}}}+\omega_6\frac{\mu^2}{\rho T}\overset{\circ}{\overline{\overline{\mathring{\mathbf{e}}\cdot\mathring{\mathbf{e}}}}},\\ \mathbf{q}^{(2)}=&\theta_1\frac{\mu^2}{\rho T}\Delta\nabla T+\theta_2\frac{\mu^2}{\rho T}\left\{\frac{D_0}{Dt}\nabla T-\nabla\mathbf{c}_0\cdot\nabla T\right\}\\&+\theta_3\frac{\mu^2}{\rho T}\nabla p\cdot\mathring{\mathbf{e}}+\theta_4\frac{\mu^2}{\rho}\nabla\cdot\mathring{\mathbf{e}}+\theta_5\frac{3\mu^2}{\rho T}\nabla T\cdot\mathring{\mathbf{e}},\end{aligned} \tag{23}$$

where $\mathbf{e}\equiv\overline{\overline{\nabla\mathbf{c}_0}}$ and the action of the operator D_0/Dt can be found in Eqs. (15.2.8) and (15.2.9) of Ref. [28]. The coefficients ω and θ are dimensionless numbers which are known for rigid spheres and some other models [28]. In terms of the reduced variables given by Eq. (14) and using $\mathbf{c}_0=u(x)\mathbf{i}$, the dimensionless expressions for $\mathbf{P}_{xx}^{BU}\equiv\mathbf{P}_{xx}^{(0)}+\mathbf{P}_{xx}^{(1)}+\mathbf{P}_{xx}^{(2)}$ and $\mathbf{q}_x^{BU}\equiv\mathbf{q}_x^{(0)}+\mathbf{q}_x^{(1)}+\mathbf{q}_x^{(2)}$ turn out to be given by

$$\begin{aligned}\mathbf{P}_{xx}^{BU\star}\equiv\frac{\mathbf{P}_{xx}^{BU}}{\rho_0u_0^2}=&\frac{\tau}{u^\star}-\sqrt{\tau}\frac{du^\star}{ds}+\left\{[2\omega_1/3-14\omega_2/9+2\omega_6/9]\right.\\&\times\left(\frac{du^\star}{ds}\right)^2-\frac{2}{3}\omega_2\frac{d}{ds}\left[u^\star\frac{d}{ds}(\tau/u^\star)\right]+\frac{2}{3}\omega_3\frac{d^2\tau}{ds^2}\\&\left.+\frac{2}{3}\omega_4\frac{u^\star}{\tau}\frac{d}{ds}(\tau/u^\star)\frac{d\tau}{ds}+\frac{2}{3}\frac{\omega_5}{\tau}\left(\frac{d\tau}{ds}\right)^2\right\}\frac{9u^\star}{16},\\ \mathbf{q}_x^{BU\star}\equiv\frac{\mathbf{q}_x^{BU}}{\rho_0u_0^3}=&\left\{[\theta_1-8\theta_2/3+2\theta_5]\left(\frac{du^\star}{ds}\right)\left(\frac{d\tau}{ds}\right)\right.\\&\left.+\frac{2}{3}[\theta_4-\theta_2]\tau\frac{d^2u^\star}{ds^2}+\frac{2\theta_3u^\star}{3}\frac{du^\star}{ds}\frac{d}{ds}(\tau/u^\star)\right\}\frac{9u^\star}{16},\end{aligned} \tag{24}$$

where for simplicity we have omitted the s dependence of $u^\star$ and τ. Substitution of Eq. (24) in Eqs. (15) and (16) leads us to a system of two differential equations of second order for $u^\star$ and τ, a system that is equivalent to a first-order system in four dimensions. In terms of $y_1(s)=u^\star(s)$, $y_2(s)=\tau(s)$, $y_3(s)=u^{\star\prime}(s)$, $y_4(s)=\tau'(s)$, the first-order system can be written as

$$\mathbf{y}'(s)=\mathbf{F}(\mathbf{y}(s),\tau_0), \tag{25}$$

where the prime denotes the derivative with respect to s and the vector field $\mathbf{F}(\mathbf{y})$ is given by

$$\mathbf{F}_1(\mathbf{y},\tau_0)=y_3,\quad \mathbf{F}_2(\mathbf{y},\tau_0)=y_4,$$

$$\mathbf{F}_3(\mathbf{y},\tau_0)=\frac{3}{2y_1^2y_2(\theta_4-\theta_2)}\left[\frac{40}{9}\tau_0y_1-\frac{16}{9}\tau_0y_1^2+\frac{8}{9}y_1-\frac{16}{9}y_1^2+\frac{8}{9}y_1^3-\frac{8}{3}y_1y_2+5y_1y_4\sqrt{y_2}-y_3y_4y_1^2\left(\theta_1-\frac{8}{3}\theta_2+\frac{2}{3}\theta_3+2\theta_5\right)+\frac{2}{3}y_1\theta_3y_3^2y_2\right],$$

$$\mathbf{F}_4(\mathbf{y},\tau_0)=\frac{1}{y_1^2y_2(c_2+c_3)}\left[\frac{16}{9}\tau_0y_1y_2+\frac{16}{9}y_1y_2-\frac{16}{9}y_1^2y_2-\frac{16}{9}y_2^2+\frac{16}{9}y_1y_2^{3/2}y_3+y_1y_2^2c_2\mathbf{F}_3(\mathbf{y},\tau_0)-y_3^2(y_1^2y_2c_1+y_2^2c_2)-y_4^2y_1^2(c_4+c_5)+y_3y_4y_1y_2(c_2+c_4)\right], \tag{26}$$

where

$$c_1=\frac{2}{3}\omega_1-\frac{14}{9}\omega_2+\frac{2}{9}\omega_6,\quad c_2=-\frac{2}{3}\omega_2,\quad c_3=\frac{2}{3}\omega_3,\quad c_4=\frac{2}{3}\omega_4,\quad c_5=\frac{2}{3}\omega_5. \tag{27}$$

The results for $\mathbf{P}^\star_{xx}$ and $\mathbf{q}^\star_x$ given by Eqs. (23) are independent of the interaction potential between the gas atoms except for the coefficients ω and θ which can in principle be computed for any interaction potential. In fact accurate values are available for Maxwell molecules and rigid spheres [14,28]. For rigid spheres, the explicit values used in this work are the following:

$$\omega_1=1.014\times4,\quad \omega_2=1.014\times2,\quad \omega_3=0.806\times3,$$

$$\omega_4=0.681,\quad \omega_6=0.928\times8,$$

$$\omega_5=\frac{3}{2}\times0.806-0.99,\quad \theta_1=\frac{45}{4}\times1.035,$$

$$\theta_2=\frac{45}{8}\times1.035,\quad \theta_3=-3\times1.03,$$

$$\theta_4=3\times0.806,\quad \theta_5=\left(\frac{105}{4}\times0.918+\frac{3}{2}\times0.806-0.15\right)\Big/3. \tag{28}$$

As in the previous case, the idea of perturbing the downstream critical point by making the velocity slightly greater and integrating to the upstream critical point is also applied for the dynamical system given by Eqs. (25) and (26) and we will come to this point later on. In Fig. 1 the projection of the solution curves in the $u^\star$-τ plane is given for $M=2$, while some details of the numerical methods used are given in the next section.

III. SIMULATIONS AND NUMERICAL METHODS

In this section we describe the results coming from the numerical calculations. Two main approaches are used. First we used Adam's method with a tolerance of value 10^{-15} to solve the differential equations given by Eqs. (25) and (26). A comparison of the ensuing results with other methods, such as the Runge-Kutta and the backward differentiation formula, has been carried out before [47,50] in the case of the Navier-Stokes equations and the Holian theory. We will not describe these numerical methods further since they have been considered in detail in the literature [39–42]. The second approach was to explore the direct simulation method as implemented by Bird [62]. There are other variants of the DSMC method, such as Nambu's method, but we decided to use Bird's implementation since it is presently more accepted and it has been validated with experimental data [63,64]. A comparison between Bird's and Nambu's methods and questions regarding the convergence of both methods to a solution of the Boltzmann equation are available in the literature [37,65]. Salomons and Mareschal [48,49] mentioned that the results from DSMC and NEMD are similar, a fact that we have corroborated for $M=134$. Therefore, we will mainly discuss the DSMC results.

Due to the advent of the computer, rather detailed information can now be obtained and analyzed. In particular, information about the distribution function can be obtained from both experiments and DSMC simulations [37,64,66]. We will compare the velocity and temperature profiles but higher order moments can also be considered, as was done in part by Salomons and Mareschal [48], who compared the viscous pressure tensor and the heat flux with numerical simulations. In the literature it is usual to take the shock thickness as a criterion to assess different theories and simulations; although a more interesting definition used for such comparisons is the asymmetry factor. However, these definitions depend only on the velocity (or the density) profile, which we believe has only partial information. Instead, in this work we explore the orbits in ''phase space,'' giving us the opportunity to see the information about both the velocity and temperature profiles. Furthermore, the orbits do not depend on the choice of the origin and so one does not have to decide between the different choices that are available in the literature. For the Burnett dynamical system we will give different projections of the solution curves since the orbits are in a four dimensional space, in contrast to the orbits of the Navier-Stokes equations which are two dimensional.

There are other numerical methods available to solve the Boltzmann equation such as Nordsiek's method [67–69]; we will give some of the results of the method for the shock wave problem. Also, we have discrete velocity models [70–72], such as the Boltzmann lattice gas or cellular automata which are very efficient from a computational point of view but we do not provide a comparison with them.

We have done calculations at a Mach number of value 2 and the results are given in Figs. 2–9. Figure 2, which gives the orbits for $M=2$ as predicted by different theories and DSMC, readily shows that the projection of the orbit given by the Burnett equations in the $u^\star$-τ plane are by and large in better agreement with the DSMC results. It is interesting to note that the Navier-Stokes and Holian theories give identi-

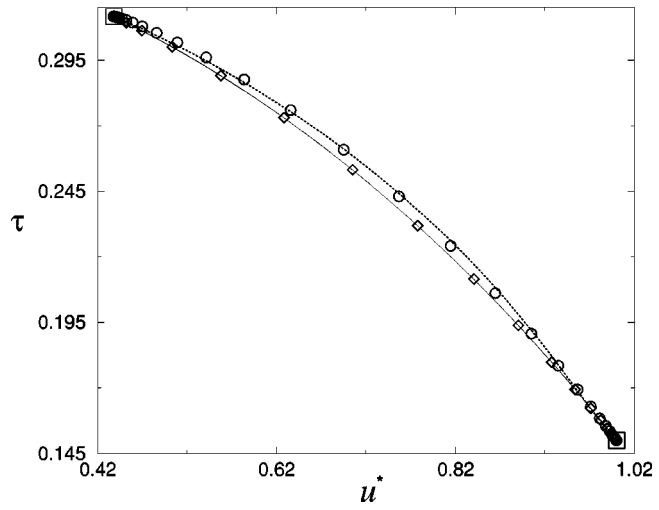

FIG. 2. Orbits in the $u^{\star}$-τ plane for $M=2$. Squares, critical points; solid line, Navier-Stokes; dotted line, Burnett; circles, DSMC; diamonds, Holian theory.

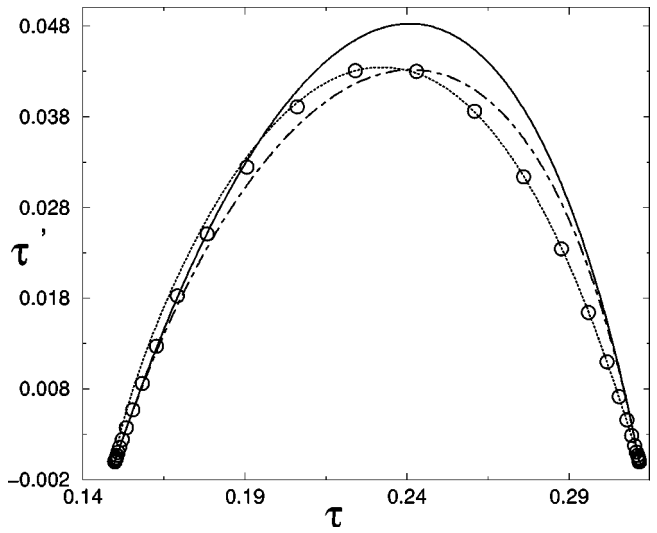

FIG. 4. Orbits in the τ-τ' plane for $M=2$. Solid line, Navier-Stokes; dotted line, Burnett; circles, DSMC; dash-dotted line, Holian theory.

cal results, a fact that can be understood by claiming that the Holian theory is a reparametrization of the Navier-Stokes equations, but, as expected, differences between these two theories will become apparent in other planes. The same conclusion, a better agreement on the whole of the Burnett equations with DSMC, can be obtained when comparing the projection of the orbits in other planes as shown in Figs. 3–5. Notice that the derivatives of $u^{\star}$ and τ for the DSMC data were evaluated using centered differences. Furthermore, the velocity and temperature profiles given in Figs. 6 and 7 show again that the Burnett equations are on the whole in better agreement with the DSMC data, and in these figures the choice of origin is taken according to Bird [37].

While the previous comparison shows that the Burnett equations are better when compared with DSMC it is convenient to carry out a more detailed comparison near the critical points. Figure 8 shows an expanded view near the upstream critical point, where the DSMC data are nearer to both the Navier-Stokes and the Holian theories. However, the dispersion exhibited by the DSMC data is not around the critical point as expected; but notice that the difference is very small. There are several possible reasons for this: (a) the first is to consider it as an indication that the heteroclinic trajectory does not exist; (b) the second would be that the upstream critical point has some structure, perhaps similar to the one given by the Burnett equations, and that the DSMC method is unable to capture the details; (c) a third is that it is necessary to consider bigger boxes in the computational scheme, and finally (d) the fourth is that it is necessary to consider longer times. We have studied some of these possibilities. As pointed out by Bird [37] the results obtained by his code are not very good if very large boxes are taken; we have indeed corroborated this fact by considering larger boxes. On the other hand, we have also considered longer times and seen that the dispersion is not substantially

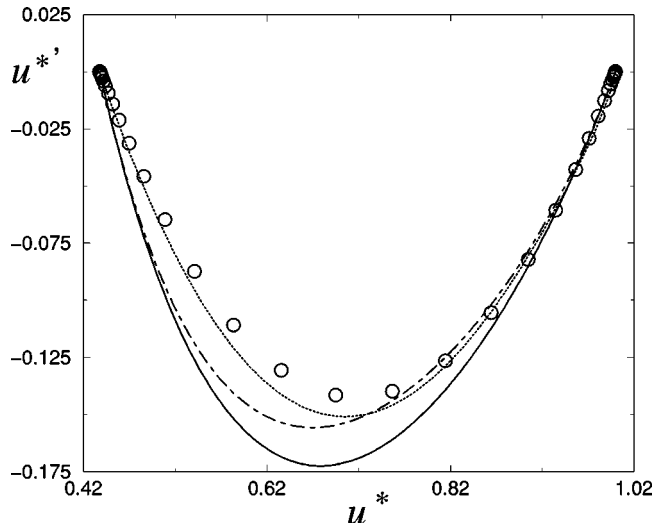

FIG. 3. Orbits in the $u^{\star}$-$u^{\star'}$ plane for $M=2$. Solid line, Navier-Stokes; dotted line, Burnett; circles, DSMC; dash-dotted line, Holian theory.

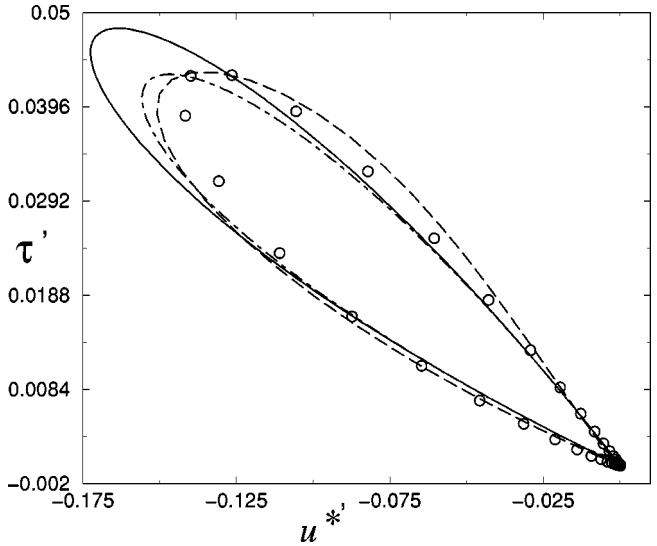

FIG. 5. Orbits in the $u^{\star'}$-τ' plane for $M=2$. Solid line, Navier-Stokes; long dashed line, Burnett; circles, DSMC; dot-dashed line, Holian theory.

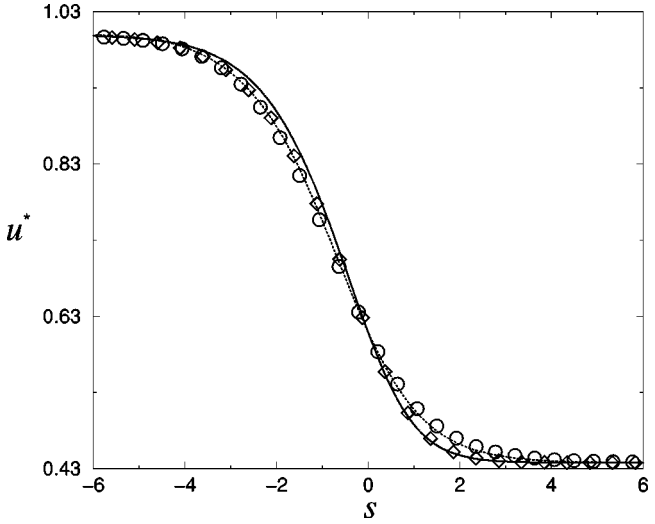

FIG. 6. Reduced velocity profiles versus the reduced length for $M=2$, $u^\star$ vs s. Solid line, Navier-Stokes; dotted line, Burnett; circles, DSMC; diamonds, Holian theory.

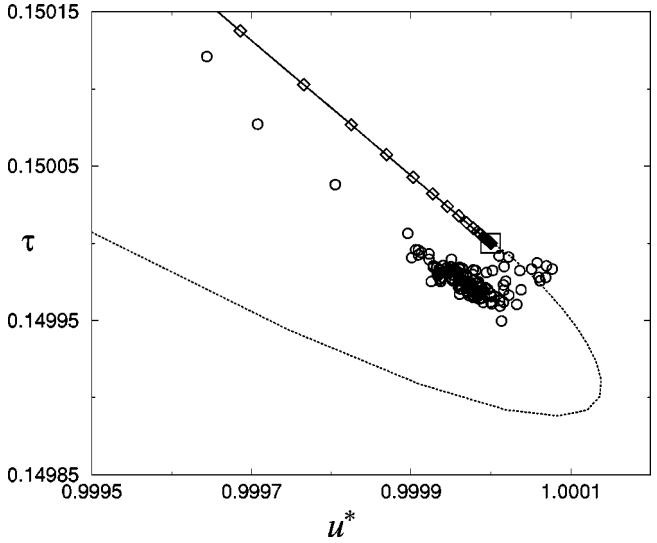

FIG. 8. Behavior of the orbits in the $u^\star$-τ plane near upflow for $M=2$. Squares, critical points; solid line, Navier-Stokes; dotted line, Burnett; circles, DSMC; diamonds, Holian theory.

changed. Pham-Van-Diep *et al.* [31] modified a code by Bird, claiming that there is a truncation error for the temperatures and this could explain the behavior observed here. A similar behavior of the DSMC data is shown at the downstream critical point and is given in Fig. 9. Notice that the conclusions previously mentioned remain valid on the whole and we would like to point out that the differences found are about the expected accuracy when using single precision arithmetic. Nevertheless, it seems strange that the fluctuations are not around the critical points. Pham-Van-Diep *et al.* [31] mentioned also that the velocity profiles are not affected by the truncation error found by them, although the DSMC velocity profiles obtained by us clearly exhibit a dispersion that on average is below the upstream critical point. As a consequence of this behavior we have been unable to calculate the asymmetry factor with confidence (see below).

Garcia and collaborators [73–75] have shown that fluctuations in DSMC results can have a physical meaning if there is a one-to-one correspondence between the number of simulated molecules and the number of real molecules (see also Ref. [37]). If DSMC simulation fails to reach one of the critical points it may be an indication that a heteroclinic trajectory does not exist. However, to be sure that this is the case, one must reduce the transverse dimensions of the simulation box, taken as 1 m^2 by Bird [37], so that the numbers of simulated molecules and real molecules are approximately equal. Such considerations would lead us to a major change in Bird's code, a task beyond the scope of this paper. Notice that, even if the dispersion of the DSMC data is around the critical point, its analysis when one can ascribe a physical meaning to it may give some information regarding the existence of a heteroclinic trajectory or the structure of an attractor in case there is one. It seems that the DSMC method and the NEMD method are by their nature unable to provide

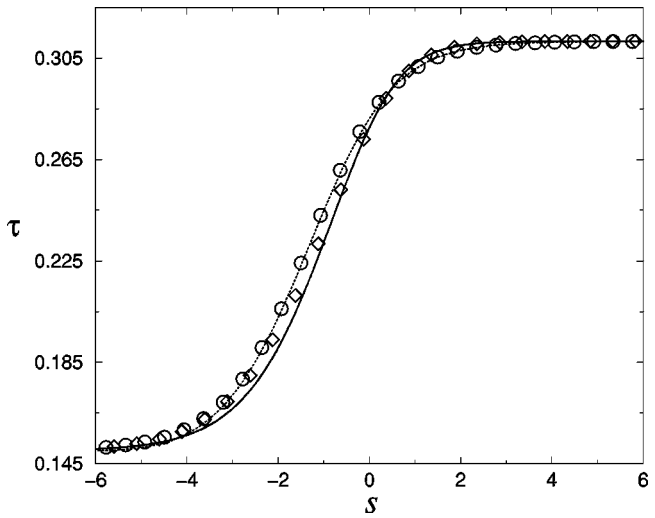

FIG. 7. Reduced temperature profiles versus the reduced lenght for $M=2$, τ vs s. Solid line, Navier-Stokes; dotted line, Burnett; circles, DSMC; diamonds, Holian theory.

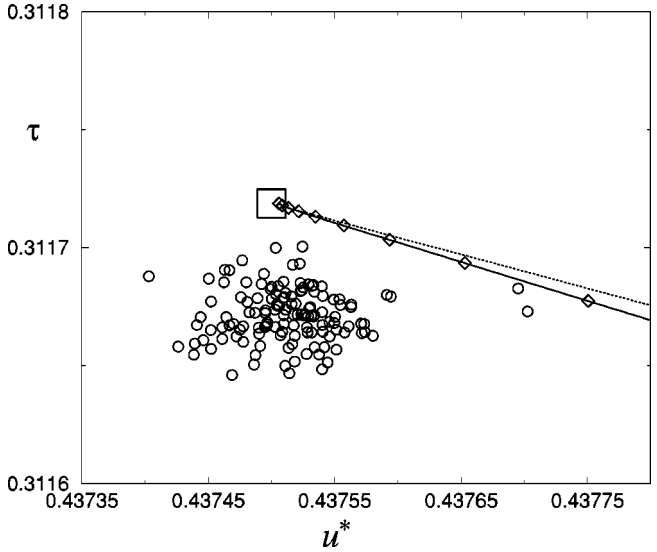

FIG. 9. Behavior of the orbits in the $u^\star$-τ plane near downflow for $M=2$. Squares, critical points; solid line, Navier-Stokes; dotted line, Burnett; circles, DSMC; diamonds, Holian theory.

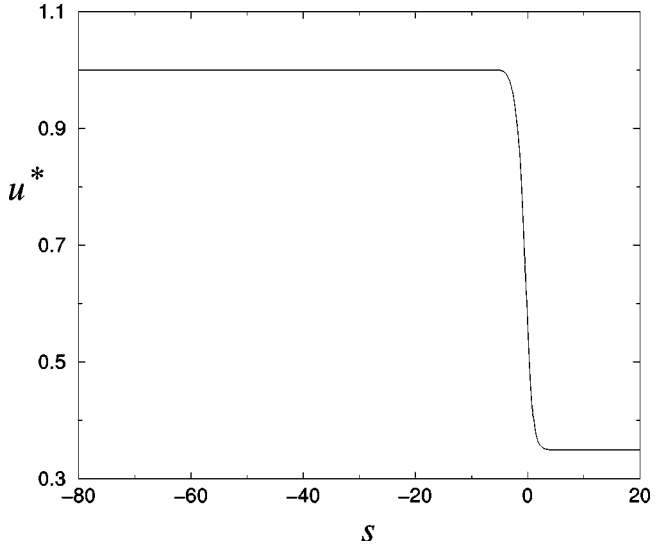

FIG. 10. Velocity profiles for the Burnett dynamical system at a Mach number of value 2.75.

clues about the existence of a heteroclinic trajectory in the mathematical sense, but this point needs further elucidation. With Adam's method we have, of course, the restriction of studying finite size boxes and in practice we have been able to carry out the integration up to $s=-10^9$. In this case the behavior of the orbits is not very interesting but represents a test for the robustness of the numerical method employed. For the DSMC method the boxes considered are about 300 mean free paths. It is also interesting to notice that in some cases the evidence for the nonexistence of a heteroclinic curve becomes apparent at large scales or through a closer inspection of the data, as shown in Figs. 10–13 for the Burnett dynamical system. The questions previously raised are irrelevant if one is interested only in the overall form of the profile, and it is our thought that at present questions regarding the existence of the heteroclinic trajectory can be tackled only with theoretical methods.

The asymemtry factor (Q_ρ) is defined by taking $L=\infty$ in

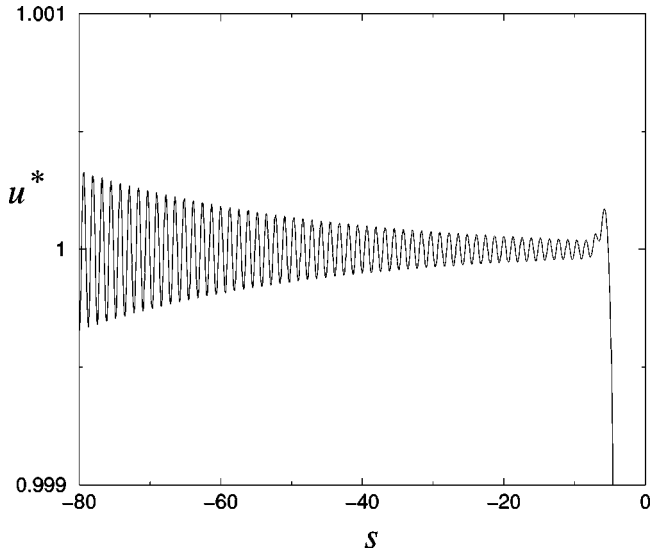

FIG. 11. Velocity profiles for the Burnett dynamical system at a Mach number of value 2.75.

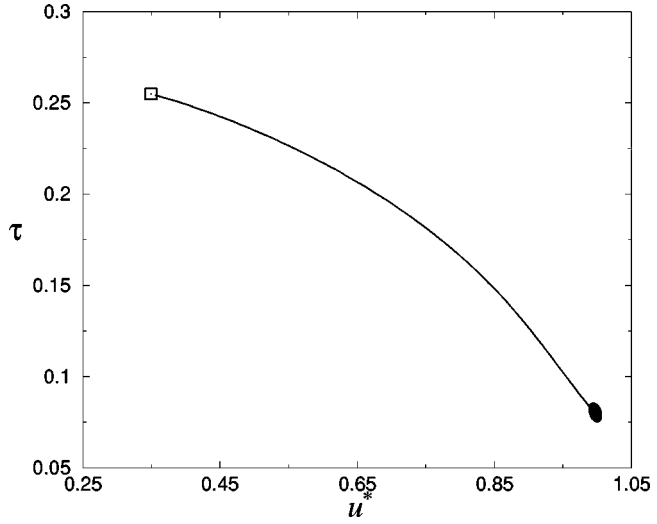

FIG. 12. Projection of the orbit for the Burnett dynamical system in the $u^\star$-τ plane for a Mach number of value 2.75. Solid line, Burnett; square, downstream critical point.

$$Q_\rho(L)\equiv\frac{\int_{-L}^{0}\rho_n(x)dx}{\int_{0}^{L}[1-\rho_n(x)]dx}, \tag{29}$$

where

$$\rho_n(x)=\frac{\rho(x)-\rho_0}{\rho_1-\rho_0}. \tag{30}$$

Here ρ is the mass density and the subscripts refer to its values downstream and upstream. In practice, one has to use a finite L to calculate the asymmetry factor but the present results taken from DSMC simulations are not of enough quality to calculate $Q_\rho(L)$ with confidence. In Fig. 14 we have considered the values reported by Pham-Van-Diep *et al.* [31] for rigid spheres. On the other hand we have provided the values for this quantity using the Navier-Stokes,

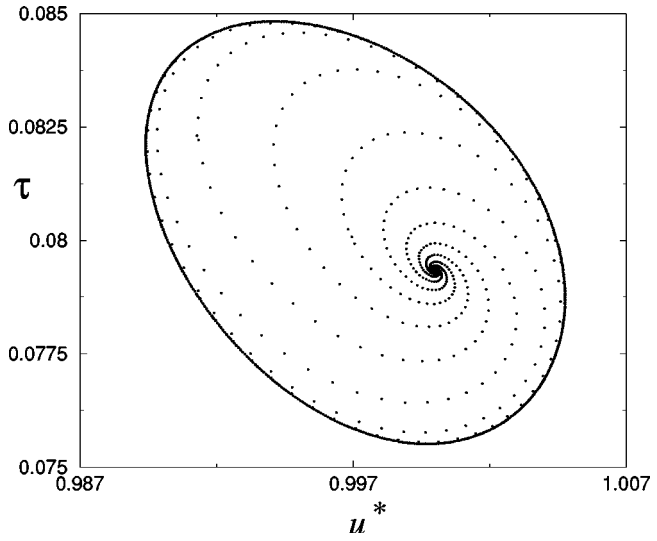

FIG. 13. Projection of the orbit for the Burnett dynamical system in the $u^\star$-τ plane for a Mach number of value 2.75 near upflow.

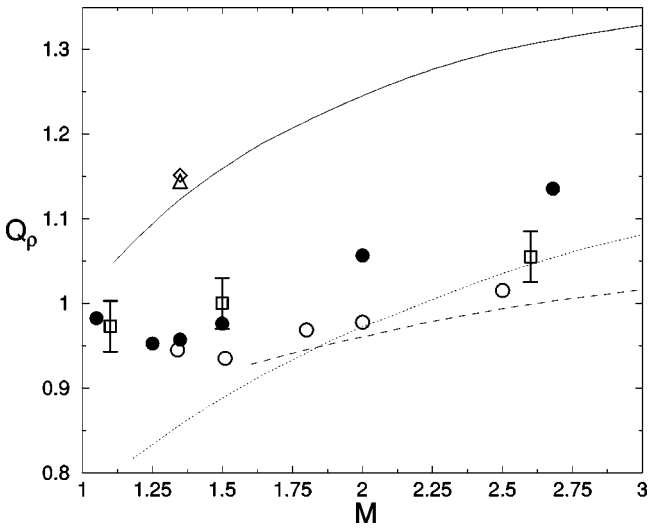

FIG. 14. Asymmetry factor versus the Mach number. Solid circles, Burnett for rigid spheres (present results); diamonds, Holian theory for rigid spheres (present results); triangles, Navier-Stokes for rigid spheres (present results); solid line, Navier-Stokes for the Maxwell model (from Alsmeyer [7]); dotted line, Nordsiek method for rigid spheres (from Alsmeyer [7]); dashed line, experimental values (from Alsmeyer [7]); squares, experimental data (from Garen *et al.* [76]); open circles, DSMC for rigid spheres (from Pham-Van-Diep *et al.* [31]).

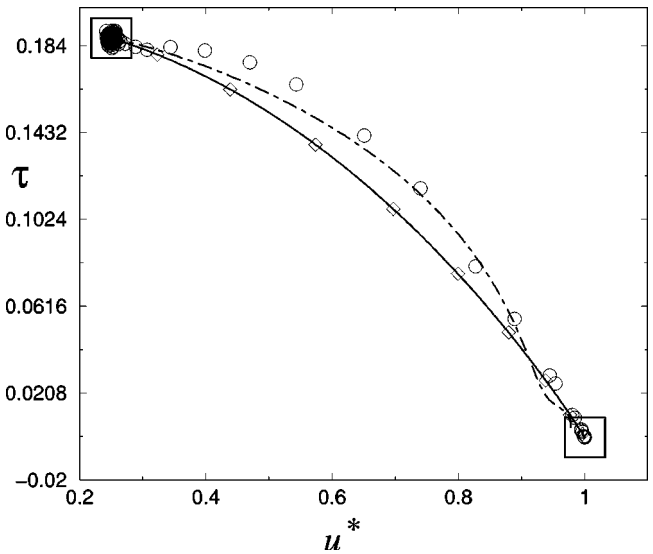

FIG. 15. Orbits in the $u^\star$-τ plane for a Mach number of value 134. Squares, critical points; solid line, Navier-Stokes; dot-dashed line, Burnett; circles, DSMC; diamonds, Holian theory.

Holian, and Burnett equations. Most of the data included in this figure were taken from Fig. 8 of the work by Alsmeyer [7] but we have restricted the Mach numbers to values lower than M_c, which is the Mach number at which the upstream critical point changes from an unstable node to a saddle (see next section). The reason is that in this region we think that the results obtained with the Burnett equations are reliable for calculating the asymmetry factor or the shock thickness. In addition we have included in Fig. 14 the experimental data of Garen *et al.* [76]. The conclusion is the same as advanced before by Alsmeyer [7] and others [31] in the sense that the Burnett equations are better than the Navier-Stokes equations for $M \leqslant 2$, although we think that there is a risk in concluding the superiority of a theory based on only one number. Coming back to Fig. 10 one may be tempted to calculate $Q_\rho(L)$ for $L=20$ for the Burnett equations, but the result is unreliable since there is no structure for the calculated orbit; the same remark applies to the shock thickness especially at higher Mach numbers.

In a previous communication [50] we provided the velocity and temperature profiles predicted by the Burnett equations for $M=\infty$ so it is instructive to see the projection of the solution curve in the $u^\star$-τ plane. The calculations were done for $M=134$ and the results can be seen in Fig. 15. Once more, the Burnett equations give on the whole a better description when compared with DSMC results. However, as we mentioned before [50], the orbits have a terminal point as clearly shown in Fig. 16; this result can be understood by claiming that the local flow cannot be extended to all the real numbers [50]. At this stage we remind the reader that the integration is carried out in the negative direction. Since the orbit terminates, we have evidence (but not proof) that there is no heteroclinic trajectory for the Burnett equations. It is possible to calculate the shock thickness but, as we pointed out before, we do not think that the calculation would be reliable since we do not get any structure for the calculated orbit; in fact, a closer inspection reveals that the derivatives become very large. On the other hand, Grad's method does not give structure for Mach numbers greater than 1.65, so the question that remains is if one would expect to have structure for all Mach numbers as happens with the Navier-Stokes equations. This question can be settled in the context of the Boltzmann equation and not using its approximations. Although we shall comment on this issue later on, we would like to make an estimation of the magnitude of the quantities involved for strong shock waves. Assume that $m=6.6\times10^{-26}$ kg and that the conditions at upflow correspond to standard values ($T=300$ K, $p=1$ atm, or about 10^5 Pa), then the sound velocity is equal to 323 m/s and the number density is about 2.5×10^{25} m^{-3}. The question that we ask is,

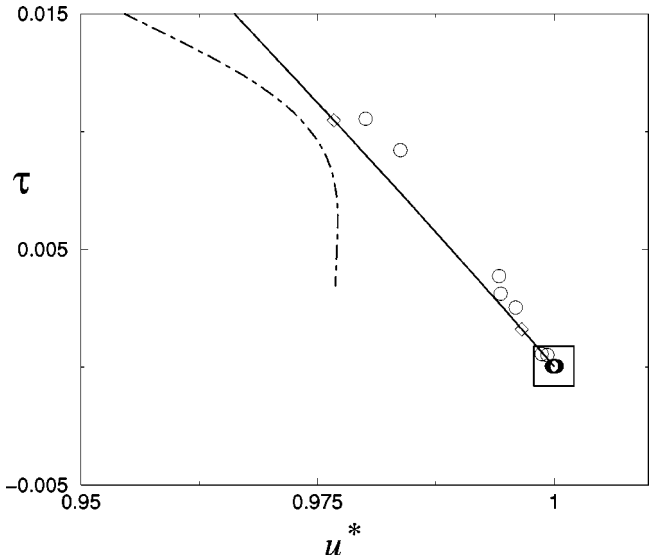

FIG. 16. Orbits in the $u^\star$-τ plane for a Mach number of value 134. Squares, critical points; solid line, Navier-Stokes; dot-dashed line, Burnett; circles, DSMC; diamonds, Holian theory.

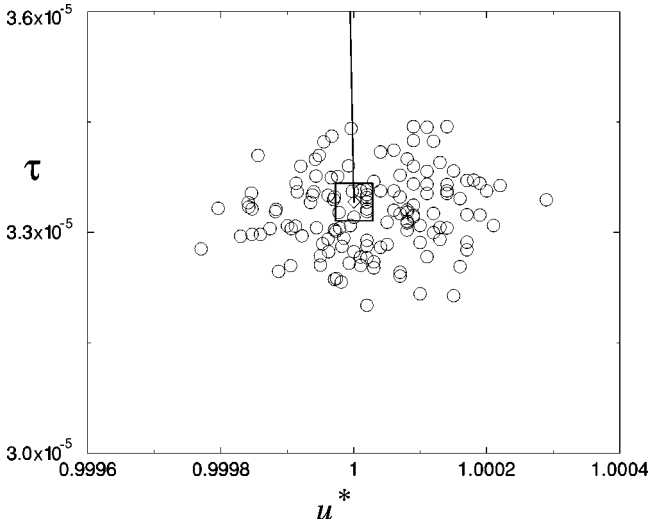

FIG. 17. Orbits in the $u^\star$-τ plane for a Mach number of value 134. Squares, critical points; solid line, Navier-Stokes; circles, DSMC; diamonds, Holian theory.

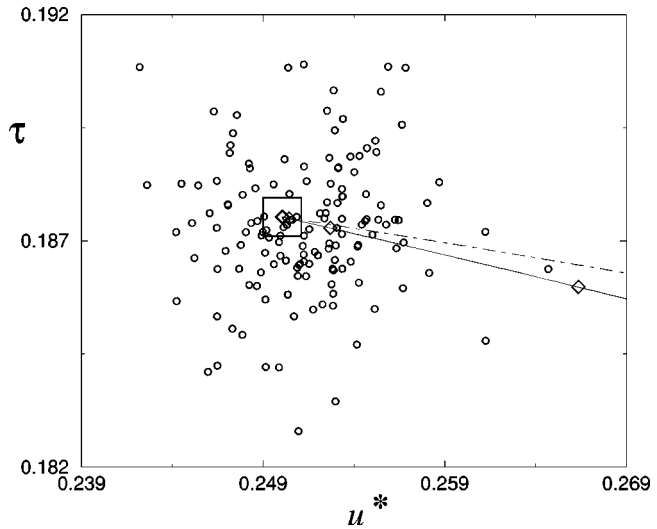

FIG. 18. Behavior near the upstream critical point in the $u^\star$-τ plane for a Mach number of value 134. Squares, critical points; solid line, Navier-Stokes; circles, DSMC; diamonds, Holian theory.

what is the temperature downstream? Notice that the number densities at downflow can be at most four times the density at upflow [see Eqs. (10) and (19)], and so the dilute condition is expected to hold provided that it holds at upflow. For $M=100$ and using the Rankine-Hugoniot equations we obtain that this temperature is of order 9×10^5 K. Clearly at such temperatures the system will be ionized. For instance, if one thinks of argon, it has an ionization energy of about 15 eV ($T\approx174\,000$ K) [77]. Thus, the question of finding structure for large Mach numbers for theories that describe monatomic gases is academic, but provides a stringent test for different theories. At a Mach number of 10 the temperature downstream is about 9500 K. The first ionization limit for argon, namely, the temperature at which 1% of the atoms are ionized, is 9500 K and 7700 K at pressures of 10^5 Pa and 10^3 Pa, respectively [78]. Therefore since the pressure at downflow is about 100 atm ($\approx10^7$ Pa) one does not need to worry about the internal structure of the gas.

It is interesing to note that for $M=134$ the dispersion exhibited by the DSMC data near both critical points exhibits the expected behavior (see Figs. 17 and 18) and is in constrast with the behavior found for $M=2$ (see Figs. 8 and 9).

The extensive comparisons performed at $M=2$ (see Figs. 2–7) show that the Burnett equations provide a substantial improvement over the Navier-Stokes equations when compared with results from DSMC simulations. The evidence based on the asymmetry factor provided by Alsmeyer [7] (see Fig. 14) shows again that the Burnett equations improve on the Navier-Stokes equations for Mach numbers near 1. Thus we can safely conclude that the Burnett equations are better than the Navier-Stokes equations for Mach numbers smaller than M_c. For large Mach numbers the Burnett equations again give a better agreement in the $u^\star$-τ plane although the derivatives of $u^\star$ and τ become large near upflow. This means that the Burnett equations are no better than the Navier-Stokes equations near upflow and the reason for this behavior is the lack of structure for the calculated orbit. We do not know yet if there is no structure for the Burnett equations when $M>M_c$, but in case this is affirmative, one would need to know if the Boltzmann equation has structure for $M>M_c$ in order to conclude that the Navier-Stokes equations are better than the Burnett equations for $M>M_c$. Even so, the calculated orbit for the Burnett dynamical system is on the whole in better agreement with results from DSMC calculations.

IV. MATHEMATICAL ANALYSIS

In this section we discuss some of the relevant mathematical aspects of the dynamical system given by Eqs. (25) and (26). The main problem here is to find the conditions under which a heteroclinic trajectory exists joining the two stationary points $(1,\tau_0,0,0)$ and $(u_1,\tau_1,0,0)$ [see Eq. (19)]. Although this question belongs to the subject of global analysis, it is important to deal first with local analysis in order to obtain the necessary conditions for the existence of a heteroclinic trajectory. The study of any nonlinear phenomenon is a difficult task and the first question that jumps into one's mind is under what conditions a nonlinear system is equivalent, under some criteria, to linearized equations, for which a great deal of information is available. There are different lines along which this question can be answered, and here we will deal with only one of its features.

A. Local analysis

In local analysis the interest is centered on the local behavior around the critical (or stationary) points and the question to answer is under what conditions the local topological behavior of the nonlinear dynamical system is equivalent to its linearized version. Let $f_\epsilon(x)$ be a vector field defined for $x\epsilon U\leqslant\mathbb{R}$, with values in $\mathbb{R}^n$, where U is an open subset and ϵ is a real number or, in general, a vector in $\mathbb{R}^k$. Also, let $x(s)$ denote a solution curve for the vector field so that

$$x'(s)=f_\epsilon(x(s)), \tag{31}$$

where the prime denotes the derivative with respect to s. If we assume that the vector field f_ϵ has continuous partial derivatives in U, $f_\epsilon\in C^1(U)$, and if x_0 is a stationary

point of f_ϵ, we can consider the solution $y(t)$ of the linearization of f_ϵ around x_0, which satisfies

$$y'(t) = Jf_\epsilon(x_0)[y(t)], \tag{32}$$

where $Jf_\epsilon(x_0)$ is the differential of f_ϵ at x_0. Alternatively, the reader may think of $Jf_\epsilon(x_0)$ as the Jacobian matrix of f_ϵ at x_0, which will be denoted by A. The prime denotes the derivative with respect to t. The solution curves for the linear system given by Eq. (32) are then given by [79,80],

$$y(t) = \exp^{(t-t_0)A} y(t_0), \tag{33}$$

where the exponentiation of a matrix is defined in terms of the series [79,80] and $y(t_0)$ denotes any given initial condition. So for linear systems the problem of finding the solution curves is equivalent to the calculation of the exponential of a matrix, and furthermore the type of eigenvalues of the matrix A determine the type of possible solution curves [79,80]. It is also important to mention that the eigenvectors corresponding to the eigenvalues of A with positive real parts generate a subspace of $\mathbb{R}^n$ called the unstable vector space E^u. The eigenvectors corresponding to eigenvalues of A with negative real parts generate a subspace called the stable vector space and denoted by E^s.

When all the eigenvalues of $Jf_\epsilon(x_0)$ have real parts different from zero, x_0 is a hyperbolic point and the Hartman [79] (or Hartman-Grobman [81]) theorem holds. This theorem establishes that for hyperbolic stationary points [79] there exists a continuous invertible map, defined in a neighborhood of x_0, which takes the solution curves of the nonlinear system, given by Eq. (31), to those of the linear system given by Eq. (32). The theorem then gives us the conditions under which the topological structure of the nonlinear system around a stationary point is the same as its linearization around the critical point. So for hyperbolic points it is enough to study the linearization around a stationary point to find the qualitative features of the solutions for the nonlinear system around the point in question. Another important theorem that holds for hyperbolic points is the stable manifold theorem [79], which states that for a hyperbolic critical point (x_0) there exist manifolds (''surfaces'') W^u and W^s, called the unstable and stable manifolds, respectively, with the same dimension as E^u and E^s, respectively, such that they are tangential to E^u and E^s at the point x_0. In the mathematical literature the stable manifold theorem is also found under the name ''Hadamard-Perron's theorem'' [82]. For nonhyperbolic points there is an analogous theorem to the stable manifold theorem which bears the name of ''the center manifold theorem'' [79,81,83].

We can now understand the following statement made by Smoller [51]; ''*There is an alternate topological way of expressing the fact that two rest points are connected by an orbit; namely, we can say that the stable manifold of one intersects the unstable manifold of the other. If this situation is to be ''structurally stable'' (i.e., remain true under small perturbations), then the sum of the dimensions of the stable and unstable manifolds must exceed that of the space. It is interesting that the entropy inequalities (24.4), allow us to explicitly compute these dimensions.*'' Two comments are pertinent at this point, but we first introduce some notation in order to make them simpler. Let x_0 and x_1 be critical points. The unstable and stable vector spaces at each of the points will be denoted by $E^u_{x_i}$ and $E^s_{x_i}$, $i=0,1$, respectively, and a similar notation will be used for the unstable and stable manifolds at each of the points. When x_0 is not a hyperbolic point then the direct sum of the previous vector spaces at each point is not $\mathbb{R}^n$ because one must introduce the ''center'' vector space E^c [79]. For simplicity we will assume that the stationary points are hyperbolic. The first remark by Smoller means that either $W^u_{x_0} \cap W^s_{x_1} \neq \varnothing$, or $W^s_{x_0} \cap W^u_{x_1} \neq \varnothing$. However, in the case of homoclinic trajectories, those for which an orbit connects a critical point with itself, it is known [84] that if the stable manifold intersects the unstable manifold transversely, the dynamics can be very complicated (homoclinic tangle), so in the case of a heteroclinic trajectory the same complications may appear unless the intersection of the manifolds is tangential. The second remark gives a criterion regarding the dimensions of the manifolds such that the heteroclinic trajectory is ''stable.'' We will refer to this as Smoller's criterion, meaning that provided that $W^u_{x_0} \cap W^s_{x_1} \neq \varnothing$ then the heteroclinic trajectory is stable if $\dim(W^u_{x_0}) + \dim(W^s_{x_1}) > n$. Finally, Smoller's last remark is not very important for us since we will be able to calculate the dimension of the unstable and stable manifolds, for each of the points, by evaluating the eigenvalues of the Jacobian matrix.

We will now apply the previous mathematical concepts and theorems to the Burnett dynamical system given by Eqs. (25) and (26). Let us first calculate the partial derivatives of the vector field given by Eq. (26), which for the first two components of the vector field can be calculated in a straightforward way. They read

$$D_3F_1(\mathbf{y},\tau_0) = 1, \quad D_4F_2(\mathbf{y},\tau_0) = 1, \tag{34}$$

where $D_k = \partial/\partial \mathbf{y}_k$ and all the other partial derivatives of F_1 and F_2 are equal to zero. The other partial derivatives are a little more complicated to calculate, the results being

$$D_1F_3(\mathbf{y},\tau_0) = -\frac{20\tau_0}{3y_1{}^2y_2(-\theta_2+\theta_4)} - \frac{4}{3y_1{}^2y_2(-\theta_2+\theta_4)} + \frac{4}{3y_2(-\theta_2+\theta_4)} + \frac{4}{y_1{}^2(-\theta_2+\theta_4)} - \frac{15y_4}{2y_1{}^2\sqrt{y_2}(-\theta_2+\theta_4)} - \frac{\theta_3 y_3{}^2}{y_1{}^2(-\theta_2+\theta_4)},$$

$$D_2F_3(\mathbf{y},\tau_0) = -\frac{15y_4}{4y_1y_2{}^{3/2}(-\theta_2+\theta_4)} - \frac{20\tau_0}{3y_1y_2{}^2(-\theta_2+\theta_4)} + \frac{8\tau_0}{3y_2{}^2(-\theta_2+\theta_4)} - \frac{4}{3y_1y_2{}^2(-\theta_2+\theta_4)} + \frac{8}{3y_2{}^2(-\theta_2+\theta_4)} - \frac{4y_1}{3y_2{}^2(-\theta_2+\theta_4)}$$

$$+\frac{3y_3y_4\theta_1}{2{y_2}^2(-\theta_2+\theta_4)}-\frac{4y_3y_4\theta_2}{{y_2}^2(-\theta_2+\theta_4)}$$

$$+\frac{y_3y_4\theta_3}{{y_2}^2(-\theta_2+\theta_4)}+\frac{3y_3y_4\theta_5}{{y_2}^2(-\theta_2+\theta_4)},$$

$$D_3F_3(\mathbf{y},\tau_0)=-\frac{3y_4\theta_1}{2y_2(-\theta_2+\theta_4)}+\frac{4y_4\theta_2}{y_2(-\theta_2+\theta_4)}$$

$$-\frac{y_4\theta_3}{y_2(-\theta_2+\theta_4)}-\frac{3y_4\theta_5}{y_2(-\theta_2+\theta_4)}$$

$$+\frac{2\theta_3y_3}{y_1(-\theta_2+\theta_4)},$$

$$D_4F_3(\mathbf{y},\tau_0)=\frac{15}{2y_1\sqrt{y_2}(-\theta_2+\theta_4)}-\frac{3y_3\theta_1}{2y_2(-\theta_2+\theta_4)}$$

$$+\frac{4y_3\theta_2}{y_2(-\theta_2+\theta_4)}-\frac{\theta_3y_3}{y_2(-\theta_2+\theta_4)}$$

$$-\frac{3y_3\theta_5}{y_2(-\theta_2+\theta_4)},$$

$$D_1F_4(\mathbf{y},\tau_0)=-\frac{16\tau_0}{9{y_1}^2(c_2+c_3)}-\frac{16}{9{y_1}^2(c_2+c_3)}$$

$$+\frac{32y_2}{9{y_1}^3(c_2+c_3)}-\frac{16\sqrt{y_2}y_3}{9{y_1}^2(c_2+c_3)}$$

$$-\frac{y_2c_2F_3(\mathbf{y},\tau_0)}{{y_1}^2(c_2+c_3)}+\frac{2y_2{y_3}^2c_2}{{y_1}^3(c_2+c_3)}$$

$$-\frac{y_3y_4c_2}{{y_1}^2(c_2+c_3)}-\frac{y_3y_4c_4}{{y_1}^2(c_2+c_3)}$$

$$+\frac{y_2c_2D_1F_3(\mathbf{y},\tau_0)}{y_1(c_2+c_3)},$$

$$D_2F_4(\mathbf{y},\tau_0)=-\frac{16}{9{y_1}^2(c_2+c_3)}+\frac{8y_3}{9y_1\sqrt{y_2}(c_2+c_3)}$$

$$+\frac{c_2F_3(\mathbf{y},\tau_0)}{y_1(c_2+c_3)}-\frac{{y_3}^2c_2}{y_1^2(c_2+c_3)}+\frac{{y_4}^2c_4}{y_2^2(c_2+c_3)}$$

$$+\frac{y_4^2c_5}{{y_2}^2(c_2+c_3)}+\frac{y_2c_2D_2F_3(\mathbf{y},\tau_0)}{y_1(c_2+c_3)},$$

$$D_3F_4(\mathbf{y},\tau_0)=\frac{16\sqrt{y_2}}{9y_1(c_2+c_3)}+\frac{y_2c_2D_3F_3(\mathbf{y},\tau_0)}{y_1(c_2+c_3)}-\frac{2y_3c_1}{c_2+c_3}$$

$$-\frac{2y_2y_3c_2}{{y_1}^2(c_2+c_3)}+\frac{y_4c_2}{y_1(c_2+c_3)}+\frac{y_4c_4}{y_1(c_2+c_3)},$$

$$D_4F_4(\mathbf{y},\tau_0)=\frac{y_2c_2D_4F_3(\mathbf{y},\tau_0)}{y_1(c_2+c_3)}-\frac{2y_4c_4}{y_2(c_2+c_3)}-\frac{2y_4c_5}{y_2(c_2+c_3)}$$

$$+\frac{y_3c_2}{y_1(c_2+c_3)}+\frac{y_3c_4}{y_1(c_2+c_3)}. \tag{35}$$

The Jacobian matrices at upflow and downflow states, denoted by JF^{up} and JF^{do}, respectively, can be obtained from Eqs. (34) and (35). Thus, the matrix elements of JF^{up} are given by

$$JF_{11}^{up}=0,\quad JF_{12}^{up}=0,\quad JF_{13}^{up}=1,$$

$$JF_{14}^{up}=0,\quad JF_{21}^{up}=0,\quad JF_{22}^{up}=0,\quad JF_{23}^{up}=0,$$

$$JF_{24}^{up}=1,\quad JF_{31}^{up}=-\frac{8}{3(\theta_4-\theta_2)},$$

$$JF_{32}^{up}=-\frac{4}{\tau_0(\theta_4-\theta_2)},\quad JF_{33}^{up}=0,$$

$$JF_{34}^{up}=\frac{15}{2\sqrt{\tau_0}(\theta_4-\theta_2)},$$

$$JF_{41}^{up}=\frac{\frac{16}{9}\tau_0^2-\frac{16}{9}\tau_0-\frac{8}{3}\tau_0^2c_2/(\theta_4-\theta_2)}{\tau_0(c_2+c_3)},$$

$$JF_{42}^{up}=\frac{-\frac{16}{9}\tau_0-4\tau_0c_2/(\theta_4-\theta_2)}{\tau_0(c_2+c_3)},\quad JF_{43}^{up}=\frac{16}{9}\frac{\sqrt{\tau_0}}{c_2+c_3},$$

$$JF_{44}^{up}=\frac{15}{2}\frac{\sqrt{\tau_0}c_2}{(\theta_4-\theta_2)(c_2+c_3)}. \tag{36}$$

For JF^{do} the first two rows are the same as for JF^{up} and the other matrix elements are given by

$$JF_{31}^{do}=\frac{128}{3(5\tau_0+1)^2(\theta_2-\theta_4)},$$

$$JF_{32}^{do}=-\frac{256}{(-14\tau_0+5\tau_0^2-3)(5\tau_0+1)(\theta_2-\theta_4)},$$

$$JF_{33}^{do}=0,\quad JF_{34}^{do}=-\frac{120}{(5\tau_0+1)\sqrt{14\tau_0-5\tau_0^2+3}(\theta_2-\theta_4)},$$

$$JF_{41}^{do}=-\frac{32}{9}\frac{12\tau_0\theta_2+3c_2\tau_0-12\tau_0\theta_4-4\theta_2-9c_2+4\theta_4}{(c_2+c_3)(5\tau_0+1)^2(\theta_2-\theta_4)},$$

$$JF_{42}^{do}=\frac{64}{9}\frac{4\theta_4+9c_2-4\theta_2}{(c_2+c_3)(5\tau_0+1)^2(\theta_2-\theta_4)},$$

$$JF_{43}^{do}=\frac{16}{9}\frac{\sqrt{14\tau_0-5\tau_0^2+3}}{(5\tau_0+1)(c_2+c_3)},$$

$$JF_{44}^{do}=-\frac{30\sqrt{14\tau_0-5\tau_0^2+3}c_2}{(\theta_2-\theta_4)(5\tau_0+1)^2(c_2+c_3)}. \tag{37}$$

The eigenvalues (λ) of the Jacobian matrix at upflow can be obtained from Eq. (36). It follows that

$$54\tau_0^{5/2}(\theta_2-\theta_4)(c_2+c_3)\lambda^4+405\tau_0^3c_2\lambda^3 + \tau_0^{5/2}[96(\theta_2-\theta_4)-360c_2-144c_3+720]\lambda^2 + \tau_0^2(720\tau_0-1104)\lambda+\tau_0^{3/2}(384-640\tau_0)=0. \tag{38}$$

Notice that in Eq. (4) of our previous work [50] we forgot to include the factor 720 that appears in the term that multiplies λ^2.

The eigenvalues of the Jacobian matrix at downflow are the solutions of a fourth-order polynomial of the form $a_0+a_1\lambda+a_2\lambda^2+a_3\lambda^3+a_4\lambda^4=0$, where

$$a_0=(196\,608-327\,680\tau_0)\sqrt{14\tau_0-5\tau_0^2+3},$$

$$a_1=125\,952\tau_0+2\,964\,480\tau_0^2-101\,376-998\,400\tau_0^3,$$

$$a_2=(49\,920\theta_4\tau_0^2+74\,880c_3\tau_0^2+2304\theta_4-167\,040\tau_0 + 19\,200\theta_2\tau_0^3+187\,200c_2\tau_0^2+33\,408c_3\tau_0-19\,200\theta_4\tau_0^3 - 17\,280+83\,520c_2\tau_0-2304\theta_2-374\,400\tau_0^2 - 49\,920\theta_2\tau_0^2+22\,272\theta_4\tau_0-22\,272\theta_2\tau_0+8640c_2 - 28\,800c_3\tau_0^3+144\,000\tau_0^3+3456c_3 - 72\,000c_2\tau_0^3)\sqrt{14\tau_0-5\tau_0^2+3},$$

$$a_3=-7290c_2-558\,900c_2\tau_0^3+546\,750c_2\tau_0^4-101\,250c_2\tau_0^5 - 474\,660c_2\tau_0^2-104\,490c_2\tau_0,$$

$$a_4=(-37\,125\theta_2c_3\tau_0^4+11\,610\theta_4c_3\tau_0^2+16\,875\theta_2c_3\tau_0^5 - 1593\theta_2c_3\tau_0-16\,875\theta_4c_2\tau_0^5-11\,610\theta_2c_2\tau_0^2+81\theta_4c_2 + 36\,450\theta_4c_3\tau_0^3-16\,875\theta_4c_3\tau_0^5+37\,125\theta_4c_3\tau_0^4 + 11\,610\theta_4c_2\tau_0^2-11\,610\theta_2c_3\tau_0^2+1593\theta_4c_2\tau_0 + 1593\theta_4c_3\tau_0+81\theta_4c_3+37\,125\theta_4c_2\tau_0^4-81\theta_2c_3 - 36\,450\theta_2c_2\tau_0^3-81\theta_2c_2-37\,125\theta_2c_2\tau_0^4 + 16\,875\theta_2c_2\tau_0^5+36\,450\theta_4c_2\tau_0^3-1593\theta_2c_2\tau_0 - 36\,450\theta_2c_3\tau_0^3)\sqrt{14\tau_0-5\tau_0^2+3}. \tag{39}$$

In Figs. 19 and 20 the corresponding real and imaginary parts of the eigenvalues obtained from Eqs. (38) and (39) are given. For the sake of clarity we have not included in the graphs the points corresponding to zero imaginary part. It is seen from Fig. 19 that the downflow is a saddle with $\dim(E^u)=3$ and $\dim(E^s)=1$. Also, for τ_0 less than 3/5 ($M=1$) and greater than approximately $\tau_0=0.485$ ($M\approx1.1123$) two eigenvalues are complex and two are real, and for $\tau_0<0.485$ ($M>1.1123$), all of them are real. In our previous communication [50] we mentioned that they were always real but the reason for this discrepancy is that we evaluated the eigenvalues for Mach numbers greater than $M=1.5$ and incorrectly interpolated the results.

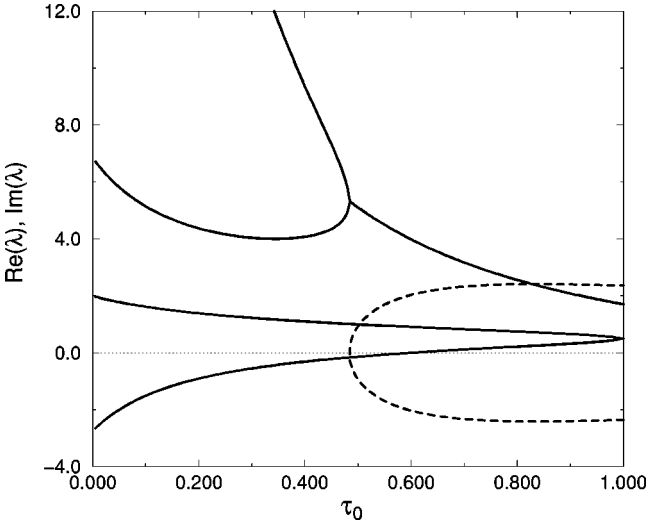

FIG. 19. Eigenvalues at downflow versus τ_0. Solid lines, real parts of the eigenvalues; dashed lines, imaginary parts of the eigenvalues. The zero imaginary parts of the eigenvalues are not shown.

For upflow (see Fig. 20) and for Mach numbers less than about $M_C=2.69$ the critical point is an unstable node and for $M>M_C$ it is a saddle with $\dim(E^s)=2$ and $\dim(E^u)=2$. So the upstream critical point has a bifurcation at M_C in which the unstable node changes to a saddle. We have investigated such a bifurcation previously and found a limit cycle [50], so that the bifurcation may be referred to as a saddle-node–Hopf bifurcation. For τ_0 less than 1 and greater than approximately 0.34 ($M=1.33$), two eigenvalues are complex and two are real. For $0<\tau_0<0.34$ ($M>1.33$) all the eigenvalues are complex.

Results similar to those described above for the eigenvalues at the two critical points were reported by Foch [29,87] for the case of the Maxwell model. Upstream the bifurcation at which the unstable node becomes a saddle appears in this case at $M=1.9$ [29].

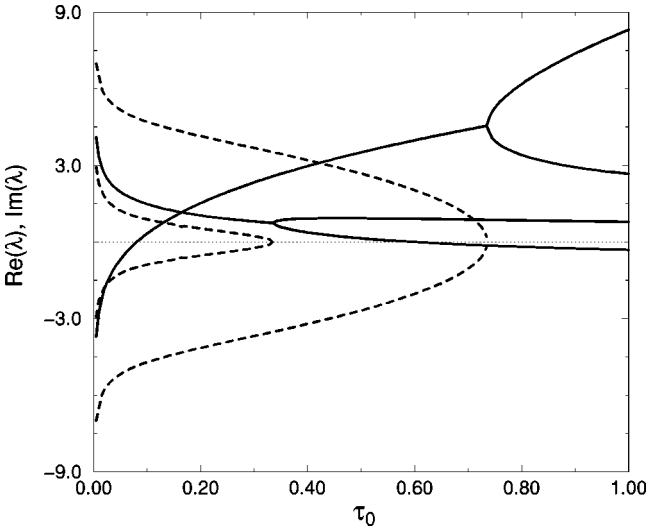

FIG. 20. Eigenvalues at upflow versus τ_0. Solid lines, real parts of the eigenvalues; dashed lines, imaginary parts of the eigenvalues. The zero imaginary parts of the eigenvalues are not shown.

Notice that for Mach numbers greater than M_C and according to Smoller's remarks mentioned previously, a structurally stable heteroclinic trajectory going from downstream to upstream is not expected, and this is consistent with both our numerical calculations and the existence of the limit cycle reported previously [50]. However, a heteroclinic trajectory from upstream to downstream does not contradict Smoller's criterion. We have been unable to find evidence of the existence of such a heteroclinic trajectory using numerical methods. Notice that, in the discussion given by Montgomery [85], such a possibility was not mentioned, perhaps due to the expectation that a curve going from upflow to downflow is not allowed because the heat flow goes from downflow to upflow. In fact such an argument has been advanced to explain the instability of some numerical methods [44,49]. In this respect it is interesting to notice that the 13-moment approximation yields a solution that goes from upstream to downstream, for Mach numbers smaller than 1.65, and so the argument could be used to invalidate the 13-moment solution. This fact was pointed out by Grad himself but apparently it has been forgotten in the recent literature. In our opinion this point deserves further consideration.

B. Global analysis

While the local analysis of the Burnett dynamical system given previously provides us with interesting information, it is unable to answer the question about the existence and/or uniqueness of a heteroclinic trajectory. Global analysis deals with such questions. There is a theorem by Montgomery [85] that focuses on such a question for the higher order gradient expansions provided by the Chapman-Enskog method, so we shall now discuss his results as applied to the Burnett equations. However, a note of caution must be given since this theorem deals only with the existence but not with the uniqueness of the heteroclinic trajectory.

There is a first requirement to apply Montgomery's result which consists in expressing the derivatives of higher order (second-order derivatives in the case of the Burnett equations) in terms of the derivatives of lower order. This part holds for the Burnett equations considered here and in fact it has been used to solve the two second-order differential equations, provided by the Burnett equations, as a first-order system in four dimensions.

Montgomery's main theorem is the following. We start with the differential equation

$$\frac{dx}{dt} = f(x,\theta), \tag{40}$$

where $x \in U \subset \mathbb{R}^n$, U is an open subset and $f: U \times [0,1] \to \mathbb{R}^n$ is a thrice differentiable function that satisfies two conditions: (a) $f(h(\theta),\theta) = f(0,\theta) = 0$, with h smooth such that $h(0) = 0$ and $(dh/d\theta)(0) \neq 0$, (b) $f_x(0,0)$ [the Jacobian matrix of $f(\cdot,\theta)$] has zero as a simple eigenvalue and no other eigenvalue has zero real part. Furthermore, if $\lambda(\theta)$ is the smooth function that gives the eigenvalues of $f_x(0,0)$ with $\lambda(0) = 0$, it is assumed that $(d\lambda/d\theta)(0) \neq 0$. Then there exists $\epsilon > 0$ and an open set V, $0 \in V \subset U$, such that for $\theta \in (0,\epsilon]$ there is a solution of Eq. (40) $x(t) \in V$ for all t and $x(t)$ connects 0 and $h(\theta)$ as t varies from $-\infty$ to $+\infty$ [if $(d\lambda/d\theta)(0) > 0$]. More details are given in the work by Montgomery [85].

Two remarks are worth noting. The first is that the two critical points given by 0 and $h(\theta)$ are the same for $\theta = 0$, which corresponds to $\tau_0 = 3/5$ $(M = 1)$ and we may take $\theta = 3/5 - \tau_0$. Second, we see that 0 is always a critical point according to Montgomery but we can always make a translation depending only on the Mach number so that one of the critical points is always 0. For example, if upflow is chosen to correspond to 0 then the function f considered by Montgomery can be defined as $f(x,\theta) = F(x + (1, \frac{3}{5} - \theta, 0, 0), \frac{3}{5} - \theta)$ [$x \equiv \mathbf{y} \in \mathbb{R}^4$; see Eq. (26)]. As we pointed out F has continuous partial derivatives of any order on a certain open set, which implies that f is in particular a thrice differential function on a certain open set. Also, $h(\theta) = (1 - \frac{5}{4}\theta, \frac{3}{5} - \theta/2 - \frac{5}{16}\theta^2, 0, 0)$ has a nonzero derivative and furthermore $f(h(\theta),\theta) = f(0,\theta) = 0$ [see Eq. (10)] so condition (a) holds.

We now need to know if condition (b) holds. Taking $\tau_0 = 3/5$ $(\theta = 0)$ in Eq. (38) we see that $\lambda = 0$ is a solution, with multiplicity 1, of $\det[f_x(0,0)] = \det(JF^{up}|_{M=1}) = 0$. Notice that the eigenvalues are not affected by the specific translation used to define f in terms of F. Furthermore, from Figs. 19 and 20 we see that $\lambda(\theta)$ has a nonzero derivative at $\theta = 0$ and no other eigenvalue has zero real part, so that Montgomery's condition (b) also holds.

We conclude that there exists a heteroclinic trajectory for the Burnett dynamical system for Mach numbers greater than 1. Although the upper limit is not known from the theorem, our numerical calculations suggest that it is equal to M_C. The mathematical concepts used by Montgomery rely on index theory and the center manifold theorem. The reader interested in having a deeper insight into these issues is referred to Montgomery's work [85], the book by Smoller [51], and Conley's monograph [86].

Finally, we end this section by summarizing the results. There exists a saddle-node–Hopf bifurcation at upflow for $M_c \approx 2.69$. In the case where $1 < M < M_c$ the upstream critical point is an unstable node and becomes a saddle for $M > M_c$, whereas the downstream critical point is always a saddle. Smoller's criterion for its existence is satisfied for $(1, M_c) \cup (M_c, \infty)$. Montgomery's theorem does not give information about the range of Mach numbers where the Burnett equations have structure; however, our numerical calculations give evidence about the existence of structure for $M \in [1, M_c)$. So far we do not know if the Burnett equations have structure for $M > M_c$, but we have found that the calculated orbit does not correspond to a heteroclinic trajectory in this case. We must not forget that for large Mach numbers the question of the existence of a heteroclinic trajectory, even for the Boltzmann equation, is academic. (One may be tempted to consider the super-Burnett or higher-order Chapman-Enskog expansions but, since they are extremely involved, it is desirable to look for alternatives [88–90].)

V. FINAL REMARKS

One of the basic questions raised by the results obtained in this work concerns the intrinsic nature of the Burnett equations. As has been pointed out in different contexts

these equations are surrounded by uncertainty that arises from various sources. The first one is their kinetic origin. They arise when the Boltzmann equation is solved through the Chapman-Enskog method and the solution is kept to terms of second order in the expansion parameter, namely, the Knudsen number. Since this number is a measure of the gradients in the system, the Burnett equations are the next order in the gradient corrections to the Navier-Stokes-Fourier equations. Two problems immediately appear: the convergence of the series, which is suspect even for small Knudsen numbers [91], and the fact that they are at odds with the second law of thermodynamics. Since 1949 [92,93] it has been known that they generate an entropy that is dependent on the gradients and, further, their entropy production is not necessarily positive definite. Other sources of uncertainly are connected with the boundary conditions they must satisfy and their frame dependence in rotatory coordinates [94], but we need not bother with all of them here. We wish here to comment on the first two of these aspects and on the possible derivation of the equations by other methods. Further discussions of the Burnett equations and more references can be found in the work by Dorfman and van Beijeren [95] and elsewhere [96].

In their work on shock waves at high Mach numbers, $M_a \approx 50$, Chapman *et al.* [32–34] emphasized that, although the results obtained with the Burnett equations substantially improve those obtained with the NSF approximation, the above mentioned theoretical questions concerning the Burnett equations need to be clarified. It is worth noting that in their work they use the Burnett equations as obtained from the Boltzmann equation using the Chapman-Enskog method. Thus, indeed, the objections raised in the preceding section hold for their results. In fact one could be even more drastic and question the validity of the Chapman-Enskog expansion itself in the presence of large gradients, which is certainly the case when $M>1$ [14]. In fact the first thing we must determine is if such equations are structurally the same regardless of the method used for their derivation. Besides the Woods [94] derivations, there are others [97] that appear to lead to the same set as that obtained via kinetic theory. Nevertheless, on account of all these facts we think that we have gained a better understanding of the Burnett equations, although their place within an irreversible thermodynamic framework and relationship with kinetic theory still remain obscure [97–100]. Due to the relative success of the Burnett equations, at least in the problem of calculating shock wave profiles for high Mach numbers [50], in the case of plane Poiseuille flow [101] and in the case of a one dimensional strongly nonisothermal gas [102], their here aspects emphasized deserve further attention.

As far as we know, the boundary conditions for the Burnett equations remain an open problem. For the Navier-Stokes equations stick boundary conditions are usually introduced, but when Knudsen's number is not small there exists a slip at the boundary and the calculation of the velocity jump is still under current research [65,103–105]. In this sense the boundary conditions for the Navier-Stokes equations are also an open question. The stick boundary conditions can be used to solve the Burnett equations but of course since they are of higher order the question of uniqueness becomes relevant. In this respect it is important to point out that there are examples [106] (Jeffery-Hamel flow) in which for a fixed Reynolds number there are an infinite number (countable) of solutions to the Navier-Stokes with stick boundary conditions. Of course, the hydrodynamic stability analysis [107] becomes a relevant choice, when there is more than one solution, one of which is stable. Nevertheless, in the case of Jeffery-Hamel flow there are regions in which there exist more than one stable solution when a linear hydrodynamic stability analysis is used [108].

As we pointed out previously [50], even when the solution to a set of equations exists (such as the Euler, NSF, or Burnett equations), it cannot be observed unless it is stable in the hydrodynamic sense, and several examples can be found in the literature [107]. There are some partial results on the hydrodynamic stability of the Euler equations for the so-called corrugational stability [4,12]. Liu [56] used constant transport coefficients in the Navier-Stokes equations to show, using the energy method [107], that the weak shock wave profiles are nonlinearly stable. We do not know if these results remain valid when the transport coeffcients are not constant, but probably this is the case. Other results about the stability of the shock wave profiles for the Navier-Stokes equations have been discussed by Smoller [51]. For the Burnett equations Bobylev's instability [109] has been, apparently, the only theoretical result concerning their hydrodynamic stability. What was shown by Bobylev is that for a system of Maxwellian molecules that is at equilibrium the Burnett equations are linearly unstable for longitudinal perturbations.

Bobylev's instability was used to explain an anomaly found by Chapman and collaborators [33,34] in the code developed by Fiscko and Chapman [32] to solve the nonstationary Burnett equations for the shock wave problem. The answer to this problem given by Chapman and collaborators was to consider either a restricted or an augmented set of equations by throwing out some of the terms given by the Burnett equations or by adding some terms which come from the super-Burnett equations. As a result of this, Chapman and collaborators obtained a stable set of equations containing higher order gradients which are linearly stable for the equilibrium state and behave well for the shock wave problem. Furthermore, their claim is that the shock wave profiles obtained by the augmented system are nearly the same as those from the Burnett equations. The last remark is doubtful in view of our own findings for Mach numbers greater than M_C, unless they are finding a solution that probably goes from upstream to downstream. This point, as well as the local analysis of their augmented system for the stationary case and the study of Bobylev's instability for realistic potentials, deserve further study. Recently [110] we have generalized Bobylev's analysis for other models and argued that Bobylev's instability can also be understood as giving a critical Knudsen number above which the Burnett equations are not valid. In other words, Bobylev's instability appears for ''large'' Knudsen numbers where the Burnett equations are expected to be invalid, so the instability found by Bobylev does not appear for small Knudsen numbers and the Burnett equations may provide an adequate description in this case. It is interesting to note that if normal modes of the form $\exp(\Omega t' + kx)$, where t' and k are a reduced time and a reduced wavelength [110], are used to perturb the equilibrium

solution considered by Bobylev [109], then for real k a linear hydrodynamic stability analysis gives the following dispersion relation:

$$18\Omega^3+69\Omega^2k^2+30\Omega k^2+18\Omega k^4 \times\left[\frac{10}{3}-\frac{4}{9}(\theta_4-\theta_2+\omega_3-\omega_2)+\frac{2\omega_2}{3}\right] +\frac{16}{3}(\omega_3-\omega_2)(\theta_4-\theta_2)\Omega k^6+45k^4+30\omega_2k^6=0. \quad (41)$$

Comparing Eq. (41) with Eqs. (38) and (27) we see that the stability of the equilibrium state and the eigenvalues at the critical points for the shock wave problem are determined only by the coefficients ω_2, ω_3, θ_3, and θ_4.

On the other hand, the problem of the structure for shock waves can be studied directly from the Boltzmann equation itself and there indeed exist several works that deal with this issue [57–59,111]. It has been proved that the Boltzmann equation, for some interaction potentials, admits structure for Mach numbers near 1 (weak shocks) but the precise value is not known [57–59]. Grad [111] suggested that the solution for the Boltzmann equation for the shock wave problem exists in the infinitely strong shock limit, and further work along these lines has been carried out by Cercignani *et al.* [22] and Caflisch [112]. As far as we understand, these works do not give a definite answer regarding the existence of structure for large Mach numbers. So the problem of the existence of a critical Mach number above which there is no structure for shock waves, at the level of the Boltzmann equation, seems to be open, as well as the ''stability'' of the solution, when it exists. We refer the reader to the literature cited above for further details.

To conclude, we would like to comment on our view of the Burnett equations. In 1963 Grad [113] made the following remark: ''On the other hand, the Burnett equations, which also belong to this theory, are viewed with grave suspicion in most quarters and have never achieved any noticeable success.'' In the light of the present and other works [7,101,102] we think that, although they may be seen with grave suspicion, it is no longer true that they have not achieved any noticeable success. The present work and others show that they are successful at least in some range of the relevant physical parameters. Bobylev's instability provides a range of Knudsen numbers for which the Burnett equations are valid [110] and therefore this instability can no longer be considered as a drawback. It would be naive to claim that they are not susceptible to improvement, as a recent work shows [101]. However, we think they provide some valuable results and therefore they can be used as a guide toward developing a more complete theory capable of dealing with situations with large gradients where the Navier-Stokes equations are expected to be inaccurate.

ACKNOWLEDGMENTS

We would like to acknowledge discussions with and/or advice from A. L. Garcia, P. Miramontes, E. Pérez-Chavela, E. Piña, and F. Sánchez-Garduño. F.J.U. wants to thank the Department of Physics of the University of Newcastle where part of this work was done and the Universidad Autónoma Metropolitana and CONACYT for providing funds for his stay at Newcastle upon Tyne. This work was financed in part by FOMES through Grant No. 98-35.15.

[1] R. Becker, Z. Phys. **8**, 321 (1922).
[2] L. H. Thomas, J. Chem. Phys. **12**, 449 (1944).
[3] D. Gilbarg and D. Paolucci, J. Ration Mech. Anal. **2**, 617 (1953).
[4] L. Landau and E. Lifshitz, *Fluid Mechanics* (Pergamon Press, Oxford, 1986).
[5] H. W. Liepmann, R. Narashima, and M. T. Chahine, Phys. Fluids **5**, 1313 (1962).
[6] Y. B. Zeldovich and Y. P. Raizer, *Physics of Shock Waves*, Vol. I (Academic Press, New York, 1966); Vol. II (1968).
[7] H. Alsmeyer, J. Fluid Mech. **74**, 497 (1976).
[8] D. Jou and D. Pavon, Phys. Rev. A **44**, 6496 (1991).
[9] J. D. Powell and J. H. Batteh, Phys. Fluids **20**, 734 (1977).
[10] C. Cercignani, in *Nonequilibrium Phenomena I: The Boltzmann Equation*, edited by J. L. Lebowitz and E. W. Montroll (North-Holland, Amsterdam, 1983), p. 121.
[11] W. C. Griffith, J. Fluid Mech. **106**, 81 (1981).
[12] S. A. Markovskii and B. V. Somov, Space Sci. Rev. **78**, 443 (1996).
[13] H. Grad, Commun. Pure Appl. Math. **5**, 257 (1952).
[14] C. S. Wang-Chang, in *Studies in Statistical Mechanics*, edited by J. de Boer and G. E. Uhlenbeck (North Holland, Amsterdam, 1970), Vol. V, p. 27.
[15] H. M. Mott-Smith, Phys. Rev. **82**, 855 (1951).
[16] M. N. Kogan, *Rarefied Gas Dynamics* (Plenum Press, New York, 1969).
[17] M. Al-Ghoul and B. C. Eu, Phys. Rev. E **56**, 2981 (1997). The introduction to this paper has valuable information concerning kinetic theoretical approaches to the study of shock waves.
[18] E. P. Muntz, Annu. Rev. Fluid Mech. **21**, 387 (1989).
[19] See Ref. [7] and literature cited therein.
[20] A. G. Bashkirov and A. V. Orlov, Phys. Rev. E **53**, R17 (1996), and references therein.
[21] Y. G. Ohr, Phys. Rev. E **57**, 1723 (1998).
[22] C. Cercignani, A. Frezzotti, and P. Grosfils, Phys. Fluids **11**, 2757 (1999). The introduction to this work has valuable information about the Mott-Smith ansatz and its variants.
[23] E. Rebhan, Phys. Rev. A **42**, 781 (1990).
[24] A. N. Gorban and I. V. Karlin, Physica A **190**, 393 (1992).
[25] L. H. Holway, Phys. Fluids **7**, 911 (1964).
[26] T. Ruggeri, Phys. Rev. E **47**, 4135 (1993).
[27] W. Weiss, Phys. Fluids **8**, 1659 (1996).
[28] S. Chapman and T. G. Cowling, *The Mathematical Theory of Non-Uniform Gases* (Cambridge University Press, Cambridge, 1970).

[29] J. D. Foch, in *The Boltzmann Equation; Theory and Applications*, edited by E. G. D. Cohen and W. Thirring (Springer-Verlag, Vienna, 1973), p. 123.
[30] J. C. Tannehill and G. R. Eisler, Phys. Fluids **19**, 9 (1976).
[31] G. C. Pham-Van-Diep, D. A. Erwin, and E. P. Muntz, J. Fluid Mech. **232**, 403 (1991), and references therein.
[32] K. A. Fiscko and D. R. Chapman, in *Rarefied Gas Dynamics*, edited by E. P. Muntz, D. P. Weaver, and D. H. Campbell, Progress in Astronautics and Aeronautics Vol. 118 (AAIA, Washington, D.C., 1989), p. 374.
[33] F. E. Lumpkin III and R. D. Chapman, J. Thermophys. Heat Transfer **6**, 419 (1992).
[34] X. Zhong, R. W. MacCormack, and D. R. Chapman, AIAA J. **31**, 1036 (1993).
[35] M. López de Haro and V. Garzó, Phys. Rev. E **52**, 5688 (1995).
[36] J. M. Montanero, M. López de Haro, V. Garzó, and A. Santos, Phys. Rev. E **60**, 7592 (1999).
[37] G. A. Bird, *Molecular Gas Dynamics and the Direct Simulation of Gas Flows* (Clarendon, Oxford, 1994).
[38] Wm. G. Hoover, *Molecular Dynamics* (Springer-Verlag, Berlin, 1986).
[39] The Numerical Algorithm Group FORTRAN library documentation has important information and many references regarding the numerical methods used in this work [The *NAG Fortran Library Manual, Mark 16* (The Numerical Algorithms Group Ltd., Oxford, UK, 1993)].
[40] W. H. Press, B. P. Flannery, S. A. Teukolski, and W. T. Vetterling, *Numerical Recipes* (Cambridge University Press, Cambridge, 1992).
[41] *Modern Numerical Methods for Ordinary Differential Equations*, edited by G. Hall and J. M. Watt (Clarendon Press, Oxford, 1976).
[42] A. L. Garcia, *Numerical Methods for Physics* (Prentice-Hall, Englewood Cliffs, NJ, 1999).
[43] A. Heck, *Introduction to* MAPLE (Springer-Verlag, Amsterdam, 1993).
[44] B. L. Holian, W. L. Hoover, B. Moran, and G. K. Straub, Phys. Rev. A **22**, 2798 (1980).
[45] B. L. Holian, Phys. Rev. A **37**, 2562 (1988).
[46] B. L. Holian, in *Microscopic Simulations of Complex Hydrodynamic Phenomena*, edited by M. Mareschal and B. L. Holian (Plenum Press, New York, 1992), p. 75.
[47] F. J. Uribe, R. M. Velasco, and L. S. García-Colín, Phys. Rev. E **58**, 3209 (1998).
[48] E. Salomons and M. Mareschal, Phys. Rev. Lett. **69**, 269 (1992).
[49] B. L. Holian, C. W. Patterson, M. Mareschal, and E. Salomons, Phys. Rev. E **47**, R24 (1993).
[50] F. J. Uribe, R. M. Velasco, and L. S. García-Colín, Phys. Rev. Lett. **81**, 2044 (1998).
[51] J. Smoller, *Shock Waves and Reaction-Diffusion Equations* (Springer-Verlag, New York, 1994).
[52] *Nonlinear Partial Differential Equations*, edited by J. A. Smoller (American Mathematical Society, Providence, R.I., 1983). Several papers in this volume deal with noncontinuous solutions for hyperbolic systems.
[53] T.-P. Liu, *Nonlinear Stability of Shock Waves for Viscous Conservation Laws* (American Mathematical Society, Providence RI, 1985).
[54] Lord Rayleigh, Proc. R. Soc. London, Ser. A **84**, 247 (1910).
[55] G. I. Taylor, Proc. R. Soc. London, Ser. A **84**, 371 (1910).
[56] T.-P. Liu, Commun. Pure Appl. Math. **39**, 565 (1986).
[57] R. E. Caflisch and B. Nicolaenko, Commun. Math. Phys. **38**, 161 (1982).
[58] R. E. Caflisch and B. Nicolaenko, in *Nonlinear Partial Differential Equations* (Ref. [52]), p. 35.
[59] R. E. Caflisch, in *Rarefied Gas Dynamics* (Ref. [32]), p. 3.
[60] A discussion of these matters can be found in G. A. Bird, *Molecular Gas Dynamics and the Direct Simulation of Gas Flows* (Ref. [37]), Sec. 2.4.
[61] D. Burnett, Proc. London Math. Soc. **39**, 385 (1935); **40**, 382 (1936).
[62] We used Bird's public domain code for the shock wave problem [37].
[63] D. A. Erwin, G. C. Pham-Van-Diep, and E. P. Muntz, Phys. Fluids **3**, 697 (1991).
[64] T. Holtz and E. P. Muntz, Phys. Fluids **26**, 2425 (1983).
[65] C. Cercignani, R. Illner, and M. Pulvirenti, *The Mathematical Theory of Dilute Gases* (Springer-Verlag, New York, 1994).
[66] G. Pham-Van-Diep, D. Erwin, and E. P. Muntz, Science **245**, 624 (1989).
[67] B. L. Hicks, S. M. Yen, and B. J. Reilly, J. Fluid Mech. **53**, 85 (1972).
[68] S. M. Yen, Annu. Rev. Fluid Mech. **16**, 67 (1984).
[69] S. M. Yen, in *Rarefied Gas Dynamics* (Ref. [32]), p. 323.
[70] R. Gatinol, Phys. Fluids **18**, 153 (1975).
[71] D. Goldstein, B. Sturtevant, and J. E. Broadwell, in *Rarefied Gas Dynamics* (Ref. [32]), p. 100. Chapter 2 of this book contains several papers dealing with discrete velocity models.
[72] A. E. Beylich, Phys. Fluids **12**, 444 (2000).
[73] A. L. Garcia, Phys. Rev. A **34**, 1454 (1986).
[74] A. L. Garcia, M. Malek Mansour, G. C. Lie, M. Mareschal, and E. Clementi, Phys. Rev. A **36**, 4348 (1987).
[75] A. L. Garcia, in *Microscopic Simulations of Complex Flows*, edited by M. Mareschal (Plenum Press, New York, 1990), p. 177.
[76] W. Garen, R. Synofzik, and G. Wortberg, in *Rarefied Gas Dynamics*, edited by J. L. Potter (AIAA, New York, 1977), p. 519.
[77] F. J. Blatt, *Modern Physics* (McGraw-Hill, Singapore, 1992).
[78] J. Kestin, K. Knierim, E. A. Mason, B. Najafi, S. T. Ro, and M. Waldman, J. Phys. Chem. Ref. Data **13**, 229 (1984).
[79] P. Glendining, *Stability, Instability, and Chaos* (Cambridge University Press, New York, 1994).
[80] M. W. Hirsch and S. Smale, *Differential Equations, Dynamical Systems, and Linear Algebra* (Academic Press, London, 1974).
[81] D. K. Arrowsmith and C. P. Place, *An Introduction to Dynamical Systems* (Cambridge University Press, Cambridge, 1990).
[82] I. V. Arnold and Yu. S. Il'yashenko, in *Encyclopedia of Mathematical Sciences*, edited by D. V. Anosov and I. V. Arnold (Springer-Verlag, Berlin, 1988), Vol. 1, p. 1.
[83] J. Guckenheimer and P. Holmes, *Nonlinear Oscillations, Dynamical Systems, and Bifurcations of Vector Fields* (Springer-Verlag, New York, 1983).
[84] S. Wiggins, *Introduction to Applied Nonlinear Dynamical Systems and Chaos* (Springer-Verlag, New York, 1990).
[85] J. T. Montgomery, Phys. Fluids **18**, 148 (1975).
[86] C. Conley, *Isolated Invariant Sets and the Morse Index* (American Mathematical Society, Providence, RI, 1972).

[87] C. E. Simon and J. D. Foch, in *Rarefied Gas Dynamics* (Ref. [76]), p. 493.
[88] P. Rosenau, Phys. Rev. A **40**, 7193 (1989).
[89] A. N. Gorban and I. V. Karlin, Phys. Rev. Lett. **77**, 282 (1996).
[90] I. V. Karlin, G. Dukek, and T. F. Nonnenmacher, Phys. Rev. E **55**, 1573 (1997).
[91] J. A. McLennan, Phys. Fluids **8**, 1580 (1965).
[92] I. Prigogine, Physica (Amsterdam) **15**, 242 (1949).
[93] S. R. deGroot and P. Manzur, *Non-Equilibrium Thermodynamics* (Dover, Mineola, NY, 1984), Chap. IX.
[94] L. C. Woods, *An Introduction to the Kinetic Theory of Gases and Magnetoplasmas* (Oxford University Press, New York, 1993).
[95] J. R. Dorfman and H. van Beijeren, in *Statistical Physics*, edited by B. J. Berne (Plenum Press, New York, 1977), p. 65.
[96] F. J. Uribe and L. S. García-Colín, Phys. Fluids A **5**, 1814 (1993).
[97] L. S. García-Colín, J. A. Robles-Domíguez, and G. Fuentes, Phys. Lett. **84A**, 169 (1984).
[98] J. A. Robles-Domínguez, B. Silva, and L. S. García-Colín, Physica A **106**, 539 (1981).
[99] L. S. García-Colín, Physica A **118**, 341 (1983).
[100] L. S. García-Colín, and M. López de Haro, J. Non-Equilib. Thermodyn. **7**, 95 (1982).
[101] F. J. Uribe and A. L. Garcia, Phys. Rev. E **60**, 4063 (1999).
[102] D. W. Mackowski, D. H. Papadopoulos, and D. E. Rosner, Phys. Fluids **11**, 2108 (1999).
[103] R. Peralta-Fabi and R. Zwanzig, J. Chem. Phys. **78**, 2525 (1983).
[104] D. L. Morris, L. Hannon, and A. L. Garcia, Phys. Rev. A **46**, 5279 (1992).
[105] J. López-Lemus and R. M. Velasco, Physica A **274**, 454 (1999).
[106] L. Rosenhead, Proc. R. Soc. London, Ser. A **175**, 436 (1940).
[107] P. G. Drazin and W. H. Reid, *Hydrodynamic Stability* (Cambridge University Press, Cambridge, 1985).
[108] F. J. Uribe, Enrique Díaz-Herrera, A. Bravo, and R. Peralta-Fabi, Phys. Fluids **9**, 2798 (1997).
[109] A. N. Bobylev, Dokl. Akad. Nauk SSSR **262**, 71 (1982) [Sov. Phys. Dokl. **27**, 29 (1982)].
[110] F. J. Uribe, R. M. Velasco, and L. S. García-Colín, Phys. Rev. E **62**, 5835 (2000).
[111] H. Grad, in *Transport Theory*, SIAM-AMS Proc. No. 1 (American Mathematical Society, Providence RI, 1969), p. 269.
[112] R. E. Caflisch, Commun. Pure Appl. Math. **38**, 529 (1985).
[113] H. Grad, Phys. Fluids **6**, 147 (1963).